Detecting climate signals in populations across life histories

Stéphanie Jenouvrier, Matthew C Long, Christophe F D Coste, Marika Holland, Marlène Gamelon, Nigel G Yoccoz, Bernt-Erik Saether

Detecting climate signals in populations across life histories

Stéphanie Jenouvrier[1], Matthew C. Long[2], Christophe F. D. Coste[3], Marika Holland[2], Marlène Gamelon[3,4], Nigel G. Yoccoz[5] and Bernt-Erik Sæther[3]

Affiliations:

1. Biology Department, Woods Hole Oceanographic Institution, Woods Hole, MA, USA
2. National Center for Atmospheric Research, Boulder, CO, USA
3. Centre for Biodiversity Dynamics, Department of Biology, Norwegian University of Science and Technology, 7491 Trondheim, Norway
4. Laboratoire de Biométrie et Biologie Évolutive, CNRS, Unité Mixte de Recherche (UMR) 5558, Université Lyon 1, Université de Lyon, Villeurbanne, France
5. Department of Arctic and Marine Biology, UiT The Arctic University of Norway, Tromsø, Norway.

E-mail addresses: Stéphanie Jenouvrier: sjenouvrier@whoi.edu; Matthew C. Long: mclong@ucar.edu; Christophe F. D. Coste: christophe.f.d.coste@ntnu.no; Marika Holland: mholland@ucar.edu; Marlène Gamelon: marlene.gamelon@univ-lyon1.fr, Nigel Yoccoz: nigel.yoccoz@uit.no; Bernt-Erik Sæther: bernt-erik.sather@ntnu.no.

Statement of authorship: SJ and ML developed the research ideas, conceptualized and designed the study. SJ performed modeling work and analyzed theoretical and empirical data. CC derived the mathematical equations. MH computed the sea ice forecasts. SJ wrote the first draft of the manuscript, and all authors contributed substantially to revisions.

Data accessibility statement: data will be be archived on two public repositories (Dryad, and Hal).

Running title: Time of emergence in populations

Keywords: Time of emergence, signal to noise, climate change, life histories, population variability, population trend, emperor penguin.

Type of article: Perspective

Length: The number of words in the abstract is 279. The number of words in the main text is $\sim$ 9000. The number of references is 90. There are 7 figures, 2 tables.

Corresponding author: Stéphanie Jenouvrier
E-mail: sjenouvrier@whoi.edu
Telephone: (508) 289-3245
Fax: (508) 457-2169
Woods Hole Oceanographic Institution
266 Woods Hole Road,
Woods Hole, MA 02543-1050
U.S.A

Abstract

Climate impacts are not always easily discerned in wild populations as our ability to detect climate change signals in populations is challenged by stochastic noise associated with climate natural variability; biotic and abiotic processes variability in ecosystem; and observation error in demographic processes. In addition, population responses to climate variability and change can be contrasted and differ among life histories, affecting the detection of anthropogenic forced change across species. To detect the impact of climate change on populations, climate-driven signals in population should be distinguished from stochastic noise. The time of emergence (ToE) identifies when the signal of anthropogenic climate change can be quantitatively distinguished from natural climate variability. This concept has been applied extensively in the climate sciences, but has not yet formally been explored in the context of population dynamics. Here, we outline a new direction for detecting climate-driven signals in population by characterizing whether climate changes are potentially beyond the year-specific stochastic variations of populations. Specifically, we present a theoretical assessment of the time of emergence of climate-driven signals in population dynamics ($\mathsf{ToE}_{\mathsf{pop}}$) to detect climate signals in populations. We identify the dependence of $\mathsf{ToE}_{\mathsf{pop}}$ on the magnitude of climate trends and variability and explore the demographic controls on $\mathsf{ToE}_{\mathsf{pop}}$. We demonstrate that different life histories (fast species vs. slow species), demographic processes (survival, reproduction) and functional relationships between climate and demographic rates, yield population dynamics that filter trends and variability in climate differently. We illustrate empirically how to detect the point in time when anthropogenic signals in populations emerge from stochastic noise for a species threatened by climate change: the emperor penguin. Finally, we propose six testable hypotheses and a road map for future research.

1 Introduction

Climate change is expected to have significant effects on biological populations [Mason *et al.*, 2019]. Many studies have assessed the influence of particular climate variables on demographic rates (e.g. survival) and population sizes [e.g. see review Gaillard *et al.*, 2013; Jenouvrier, 2013]. However, while the primacy of climate influence is commonly accepted, specific detection and attribution of population trends to anthropogenic changes in climate is complicated by substantial stochastic noise related to observation error (i.e., errors due to measurement imprecision) and process error in biological processes (i.e., unexplained variation in true abundance driven by unobserved biotic such as species interactions or abiotic processes such as habitat degradation, explotation ressources...) and climate variability [Che-Castaldo *et al.*, 2017; Parmesan *et al.*, 2013].

Climate variability is an important characteristic of climate change and a driver of population dynamics [Boyce *et al.*, 2006; Vázquez *et al.*, 2015], that may occlude the population response to the underlying climate change signal. Climate variability is a noise from unforced variability generated internally within the climate system (e.g. weather) or associated with external forces to the climate system (e.g. volcanoes, Mann *et al.* [2021]), referred as natural variability. Natural variability in the climate system occurs over a broad range of temporal and spatial scales, with spectral properties in the seasonal, interannual to decadal bands. It arises from different sources, including variations that are (1) driven by a periodic external forcing, like the diurnal or the seasonal cycle of insolation, (2) due to the non-linear interplay of feedbacks within the climate system, such as coupled mode of variability (e.g. El Niño-Southern Oscillation, North Atlantic Oscillation, Pacific Decadal Oscillation), and (3) associated with random fluctuations in the external or internal climate system [Ghil, 2002]. In addition, climate change is characterized by an anthropogenic climate change signal. This secular trend is the deterministic response of the climate system to an external forcing driven by anthropogenic emissions of

greenhouse gases and changes in land use. Hence, the detection of anthropogenic forced change is a signal to noise problem.

To detect and attribute the threats to a species posed by climate, climate-driven signals in population should be distinguished from stochastic noise. The concept of time of emergence (ToE) exactly does that: it identifies when the signal of anthropogenic climate change can be formally distinguished from noise associated with natural variability. In climate science, the ToE has been studied extensively [Hawkins *et al.*, 2020; Hawkins & Sutton, 2012]. It is used to detect climatic changes and to describe whether climate changes are potentially beyond the known natural environmental variability of ecosystems [Giorgi & Bi, 2009; Mahlstein *et al.*, 2013].

Although, this concept of ToE has yet to be formally applied to ecological time series, some studies have quantified when novel climate conditions relevant for ecological processes will emerge from natural variability. For example, Beaumont *et al.* [2011] have characterized the standard deviation (SD) of surface air temperature for a baseline period (1961-1990) and then evaluated the number of months that the temperature exceeds 2 SDs by 2070 for various ecoregions of exceptional biodiversity. They found that more than 83% of terrestrial and freshwater ecoregions will be exposed to temperature exceeding 2 SDs by 2070.

The ToE explicitly characterizes the point in time when anthropogenic climate change can be formally distinguished from noise associated with natural variability. Hence, it informs on how fast changes exceed natural variability and can help prioritize decisions about when, where and for which conservation and management actions may be necessary. It is a relative measure as it depends on the threshold at which climate change is said to emerge based on assumptions about management's ability. Some studies have characterized explicitly the ToE of ecosystem drivers in marine ecosystems [Henson *et al.*, 2017; Schlunegger *et al.*, 2020]. For example, Henson *et al.* [2017] found that climate change signals of pH and SST emerge rapidly while climate change trends in interior oxygen con-

tent and primary productivity emerge later. In terrestrial ecosystems, Rojas *et al.* [2019] focused on the timing when the precipitation changes will emerge outside the range of natural variability during the 21th century relevant for agricultural activities. They found early timing of emergence in precipitation trends for the production regions of four major crops (wheat, soybean, rice, and maize) even under a low-emission scenario. Sorte *et al.* [2019] characterized the seasonal and spatial variations in the emergence of novel climates characterized by precipitation, minimum and maximum temperature, along the migration routes of 77 passerine bird species. They found that earlier ToE occur for migrants that winter within the tropics. However, none of these studies have applied directly the concept of ToE to time series of population dynamics.

Here, we apply the concept of ToE to characterize climate-driven signals in population dynamics. We present a new perspective on detecting climate-related impacts in populations by characterizing the ToE in population growth rate (herefater, $\mathsf{ToE}_{\mathsf{pop}}$), the point in time when climate-driven signals in population dynamics can be quantitatively distinguished from noise associated with year-specific stochastic variations in population growth rates (Fig. 1). While in climate science the noise is associated with climate natural variability, applying this approach to population dynamics does not exclude other sources of noise (e.g. observation and process errors).

For species threatened by climate change, $\mathsf{ToE}_{\mathsf{pop}}$ can represent the time at which the population will decline to a level below its historical variability. This point in time potentially corresponds to the time at which the species will be exposed to high extinction risk, to the time at which individuals will migrate massively to track ecological niches, or to the time at which individuals may have to adapt to new conditions through evolutionary adaptations. The earlier the $\mathsf{ToE}_{\mathsf{pop}}$ occurs, the faster novel conditions emerge out of the natural range of variability, the faster the population will reach a non-historical level, with less time for the organisms to adapt or migrate. The $\mathsf{ToE}_{\mathsf{pop}}$ is one illustrative metric that acknowledges the dual role of natural variability and an anthropogenic cli-

mate change signal, also useful for populations increasing under climate change [Román-Palacios & Wiens, 2020; Stephens *et al.*, 2016]. Importantly, ToE allows meaningful comparative studies of when the signal of anthropogenic climate change emerges from natural variability across ecosystem drivers [Henson *et al.*, 2017], species [Sorte *et al.*, 2019], ecosystems [Beaumont *et al.*, 2011] and for future socio-economic processes relevant for climate mitigation [Schlunegger *et al.*, 2020].

From a conceptual viewpoint, $\mathsf{ToE}_{\mathsf{pop}}$ occurs earlier when the slope of the population climate-driven trend is larger and when the population variability is smaller (Fig. 1). Both the population climate-driven trend and variability depend on the species' life history and the functional relationships between climate and the demographic rates (Barraquand & Yoccoz [2013], section 2). After briefly reviewing the time of emergence in climate (section 3), we characterize and compare the time of emergence of climate-driven signals in population dynamics in a theoretical context to address five questions (section 4):

- How does $\mathsf{ToE}_{\mathsf{pop}}$ in populations relate to ToE in climate?
- How does $\mathsf{ToE}_{\mathsf{pop}}$ vary across life histories (e.g. slow- fast species)?
- How does $\mathsf{ToE}_{\mathsf{pop}}$ vary across demographic processes (e.g. survival, reproduction)?
- How does $\mathsf{ToE}_{\mathsf{pop}}$ vary among different functional relationship between climate and demographic rates?
- Do some species, demographic processes or functional relationship magnify the signal of anthropogenic climate change?

We find that different life histories (e.g., long vs. short-lived species) and demographic processes by which climate affects the population (i.e., through survival, reproduction) provide different "scale-dependent" filters so that some life histories magnify signal-to-noise ratios while other demographic dynamics prolong $\mathsf{ToE}_{\mathsf{pop}}$. Furthermore, to illustrate our theoretical results, we quantify the $\mathsf{ToE}_{\mathsf{pop}}$ of an iconic species endangered by climate

change: the emperor penguin (*Aptenodytes forsteri*) [Jenouvrier *et al.*, 2021] (section 5). Finally, we propose a set of six testable hypotheses based on the patterns of ToE in climate (hereafter $\mathsf{ToE}_{\mathsf{climate}}$) and the demographic processes across life histories and propose a road map for future studies on the $\mathsf{ToE}_{\mathsf{pop}}$ (section 6).

2 Conceptual model of the time of emergence in climate and in population

Both the climate-driven trend in population growth rate and its year-specific stochastic variations are related to climate trend and variability (section 2.1, Fig. 1). However, we still lack a theoretical understanding on how the population trend and variability respond to climate in a non-stationary environment. In a stochastic stationary environment, however, we show here that the variance in annual population growth rates $\mathsf{var}(\lambda)$ is linearly related to the climate variance σ^2, and depends also on the sensitivity of the population growth rate to climate $\frac{\partial \lambda}{\partial C}$ (section 2.2).

2.1 Factors influencing the $\mathsf{ToE}_{\mathsf{pop}}$

The time of emergence is generally characterized from a time series by comparing (1) the time varying signal, $T(t)$ estimated as the long term monotonic trend (red trend on figure 1) and (2) the noise based on the range of natural variability (e.g., the standard deviation) over some historical period (variations of the black time series on figure 1). Figure 2 illustrates the signal threshold method, where the time of emergence is the first year when the projected future state of a variable crosses a pre-defined emergence threshold based on the historical variations. For example, the projected future state can be depicted by the gray envelope of future projections (red lines on Figs. 1, 2) under a specific forcing scenarios based on a range of emissions of greenhouse gases (GHGs), while the emergence threshold can be determined from the gray envelope of historical projections (black lines on Figs. 1, 2)).

In impact studies, the emergence threshold (e.g. horizontal lines on Figs. 1, 2) can be

interpreted as thresholds beyond which management-relevant impacts must occur and depend on the management sensitivity to changes in climate conditions. Indeed, emergence thresholds are not necessarily set at the extreme 2.5% high or 2.5% low of the range of historical population variations ($\sim$ 2SD) usually used in risk impact studies but can be set at any thresholds at which the decline or increase in population is perceived as unsustainable. For example, high management sensitivity threshold may be desirable for increasing species, whereby management actions are triggered by the e.g. 75% percentile of population growth distribution during the baseline period.

Figure 2 shows that the time of emergence in populations vary among species. From a conceptual viewpoint, this depends on the sensitivity of the population growth rate to climate: $\frac{\partial \lambda}{\partial C}$ (Fig. 1). This sensitivity can be decomposed into two main components. First, it depends on the sensitivity of the demographic rates themselves θ_i (e.g. survival, reproduction) to climate $\frac{\partial \theta_i}{\partial C}$ (panel 1 in the demographic rates box on Fig. 1). Therefore, the functional relationships between climate and the demographic rates likely play a key role in the sensitivity of the population growth rate to climate. Second, $\frac{\partial \lambda}{\partial C}$ depends on the sensitivity of the population growth rate to demographic rates $\frac{\partial \lambda}{\partial \theta_i}$ (panel 2 in the demographic rates box on Fig. 1). The later is influenced by the species' life cycle and thus species' life history [Saether & Bakke, 2000]. For instance, the demographic buffering hypothesis posits that in long-lived species, adult survival is expected to be buffered against environmental changes (environmental canalization sensu Gaillard & Yoccoz [2003]) and reproduction is expected to be more variable with stronger functional relationships with climate. The opposite patterns are expected in short-lived species (see Hilde *et al.* [2020] for a review). Therefore, demographic rates of species with contrasting life histories are expected to be differently influenced by climate, influencing in turn the sensitivity of the population growth rate to climate, the variance in annual population growth rates and the climate-driven change in population.

2.2 Population variability in a stationary environment

In this section, we build on previous theoretical studies [Engen *et al.*, 2005; Morris *et al.*, 2008] to show how the variance in annual population growth rates depends on the variance in climate σ^2, and the functional relationship between climate $\overline{C}$ and demographic rates, assuming a stationary environment: its mean $\overline{C}$ and variance σ^2 do not vary over time. For a structured population model of the form $\mathbf{n}_{t+1} = \mathbf{A}_t\mathbf{n}_t$ (see section 4) in a stationary environment characterized by small variations, the environmental variance of the population growth rate λ_t (such that $N_{t+1} = \lambda_t N_t$) can be approximated (first degree Taylor approximation) by [see Engen *et al.*, 1998, 2005]:

$$\mathsf{var}(\lambda_t) = \sum_{i,j} \frac{\partial\lambda}{\partial\theta_{i_{\theta_i=\overline{\theta_i}}}} \frac{\partial\lambda}{\partial\theta_{i_{\theta_j=\overline{\theta_j}}}} \mathsf{Cov}(\theta_i, \theta_j) \tag{1}$$

with $\overline{\theta}$, the vector of mean demographic parameters including fertility, survival of juveniles and adult and maturation rates (Table 1). This variance is important as it influences the long-term stochastic growth rate of the population:

$$\log\lambda_s = \lim_{T\to\infty} \frac{1}{T} \log\|\mathbf{A}_{T-1}\cdots\mathbf{A}_0 n(0)\|. \tag{2}$$

Let us assume that the environment affects only one demographic rate, θ_i (the other rates θ_j remain constant over time), then Eq 1 simplifies as:

$$\mathsf{var}(\lambda_t) = \left(\frac{\partial\lambda}{\partial\theta_{i_{\theta_i=\overline{\theta_i}}}}\right)^2 \mathsf{var}(\theta_{it}). \tag{3}$$

The demographic rate θ_i is a function of a climatic variable C_t. θ_i is also affected by other unknown variables generating environmental stochasticity ϵ, such as observation and process errors. ϵ is a stochastic environmental noise of mean 0, and variance $\mathsf{var}(\epsilon_t)$ and is considered as an additional variability independent from C. For example, let's

assume that θ_i is an inverse logit function of a linear function of C:

$$\theta_{it} = \theta_i(C_t, \epsilon_t) = g(y = \beta_0 C_t + \beta_1 + \epsilon_t), \tag{4}$$

where β_0 and β_1 are the constant regression coefficient of the functional relationship between climate and the demographic rate (FIG 1); g is the inverse logit link function so that $\theta_i \in [0\ 1]$. Applying the second order Taylor expansion, the variance of the demographic rate θ_i is:

$$\mathsf{var}(\theta_{it}) \approx (g'(\overline{y}))^2 \mathsf{var}(y) = \left(\frac{\partial \theta_i}{\partial C_{C=\overline{C}}}\right)^2 (\beta_0^2 \sigma^2 + \mathsf{var}(\epsilon_t)^2) \tag{5}$$

with σ^2 the variance of the climatic variable C and

$$\frac{\partial \theta_i}{\partial C_{C=\overline{C}}} = y' \frac{\exp(-y)}{(1+\exp(-y))^2} = \beta_0 \frac{\exp(-\beta_0 \overline{C} - \beta)}{(1+\exp(-\beta_0 \overline{C} - \beta_1))^2} \tag{6}$$

.

Hence Eq 3 can be simplified as:

$$\mathsf{var}(\lambda_t) = \left(\frac{\partial \lambda}{\partial \theta_{i_{\theta_i=\overline{\theta_i}}}}\right)^2 \left(\frac{\partial \theta_i}{\partial C_{C=\overline{C}}}\right)^2 (\beta_0^2 \sigma^2 + \mathsf{var}(\epsilon_t)^2). \tag{7}$$

Applying the derivative chain rule and assuming $\epsilon = 0$, i.e., that the demographic rate θ_i is a deterministic function of climate, like in our simulations, we obtain:

$$\mathsf{var}(\lambda_t) = \beta_0^2 \sigma^2 \left(\frac{\partial \lambda}{\partial C_{C=\overline{C}}}\right)^2 \tag{8}$$

Hence the year-specific stochastic variation depends on climate internal variability σ^2, the stochastic environmental variability, as well as the sensitivity of the population growth rate to the demographic rate and the sensitivity of the demographic rate to climate in a stationary environment that both define the overall the sensitivity of the population growth rate to climate.

In a non-stationary environment (Fig. 1), $\overline{C}$ is changing, and $\mathsf{var}(\lambda)$ varies, in general, non-linearly with $\overline{C}$ depending on the sensitivity of the population growth rate to climate $\left(\frac{\partial \lambda}{\partial C}\right)$ (see Supplementary Appendix 1 and Fig. 1), this latter also influencing the population trend. Hence, it is extremely difficult to posit a priory how $\mathsf{ToE}_{\mathsf{pop}}$ will vary with the signal and noise in climate across life histories and demographic processes for various functional relationship between climate and demographic rates. In section 4 we use a simulation framework to answer our five questions posed in the introduction, and discuss six testable hypotheses in section 6.

3 Time of emergence in climate

The concept of $\mathsf{ToE}_{\mathsf{climate}}$ has been discussed for several decades in the climate sciences with studies attempting to detect the carbon dioxide warming signal published more than 80 years ago ([Callendar, 1938; Revelle & Suess, 1957], see review in Hawkins *et al.* [2020]). The time of emergence has been characterized in temperature [Mahlstein *et al.*, 2011], precipitation [Giorgi & Bi, 2009], climate extremes [King *et al.*, 2015], in sea level [Lyu *et al.*, 2014], in Arctic climate [Landrum & Holland, 2020] and biogeochemical variables [Henson *et al.*, 2017; Schlunegger *et al.*, 2020].

Different methods have been used to quantify $\mathsf{ToE}_{\mathsf{climate}}$, most of them using climate model simulations (but see Hawkins *et al.* [2020] for an application using observation of temperature). The common methods for estimating $\mathsf{ToE}_{\mathsf{climate}}$ are the signal threshold method (section 2), and the signal-to-noise ratio method with a particular cutoff [Hawkins & Sutton, 2012] with a variant of this approach being the identification of the signal-to-noise ratio using a predefined threshold across multiple consecutive years (refereed as the exceedance threshold) [Mora *et al.*, 2013]. Different criterion have been used to ensures that the trend exceeds 95% of the values in the noise, such as a ratio 2SD/Trend [Henson *et al.*, 2017]. Various statistical methods have been developed, from statistical test to assess for significant differences between time periods [Zappa *et al.*, 2015], estimation

of the standard error of the regression to estimate the lead-time required for a linear trend to emerge from natural variability [Mahlstein *et al.*, 2012], development of hierarchical statistical state-space model [Barnhart *et al.*, 2016] or artificial neural networks [Barnes *et al.*, 2018].

Recently, the availability of large ensembles have permitted climatologists to compute emergence threshold from the distribution of these large ensemble to formally consider the uncertainty in the forced response due to natural climate variability [Barnhart *et al.*, 2016]. Large ensembles represents a set of climate simulations to characterize the natural climate variability by simulating several members subject to the same radiative forcing scenario but beginning from slightly different initial atmospheric state within a particular climate model [Kay *et al.*, 2015].

Here, we use signal threshold method (section 2) based on a large ensemble by constructing prediction interval of the climate and population projections, and estimate the time taken by the system to exit the background of natural variability [Barnhart *et al.*, 2016]. For example, the left part of Figure 2 shows the 95% prediction interval of the climate in gray. Here, $\mathsf{ToE}_{\mathsf{climate}}$ is the time when the projected future conditions under the influence of climate change, "forced conditions" (red lines), exceeds a pre-defined threshold for emergence from the projected historical unperturbed conditions (gray area, with the horizontal line illustrating the baseline threshold at which climate change is defined to emerge).

The emergence thresholds are typically based on the percentile of the distribution of the historical and forced projections. They define the prediction intervals at which the signal of climate change emerges from the natural climate variability. We present the results for one threshold of wide confidence envelope with a 95% prediction interval based on emergence thresholds defined by the 2.5 or 97.5 percentile values of the distribution, where impacts are triggered by the extreme historical conditions only. The analysis with a narrow confidence envelope with emergence thresholds defined by the 20 or 80 percentile

values of the confidence interval is shown in appendix (Fig S 4). In that case, the system is likely highly sensitive to climate as severe impacts are thought to occur for lower percentile of the climate conditions distribution experienced during the historical run. Our results are qualitatively the same between these two thresholds.

In our simulations, we construct a large ensemble of climate time series for both the historical and forced environment for various natural climate variability (σ^2) and warming trends (α). Specifically, the historical climate time series are obtained by sampling into a normal distribution – centered on a zero mean and with a specific standard deviation σ – with independent draws each year (i.e. Independent and Identically Distributed random variables (IID)). The forced climate time series are calculated by adding to this natural variability a linear trend of slope α. In that context, this ToE calculation in an IID environment is directly related to the signal-to-noise ratio: $ToE = \frac{2P}{SNratio}$ with P the climate value corresponding the threshold of the prediction interval.

In our theoretical study, we explore a range of parameters consistent with the observed standard deviation of the inter-annual temperature variability (Fig 1 of Hawkins & Sutton [2012]) and the projected climate warming by 2100 (IPCC), with $\sigma_C \in [0.2\ 1.5]$ and $\alpha_C \in [0.01\ 0.15]$ (Fig. 2). In our empirical example, we used 40-members from the Community Earth System Model Large Ensemble (CESM-LE) to characterize the confidence envelope of sea ice, hence the $\mathsf{ToE}_{\mathsf{climate}}$ and $\mathsf{ToE}_{\mathsf{pop}}$.

4 Time of emergence in populations

4.1 Population projections

For each of the four species, the population dynamic is projected using a simple two-stage climate-dependent population matrix model that permits to explore some of the diversity of life cycles along the slow-fast continuum of life histories [Caswell, 2001; Neubert & Caswell, 2000]. The model distinguishes non-reproducing juveniles and reproducing adults (see life cycle on Fig. 1). The population is projected from year *t* to year *t+1*

by:

$$\mathbf{n_{t+1}} = \mathbf{A}(\theta[(\mathbf{C_t})])\mathbf{n_t} \tag{9}$$

with $\mathbf{n_t}$ the population vector made of the abundances of juveniles and adults and $\mathbf{A}$ the population transition matrix including demographic rates $\theta[(\mathbf{C_t})]$ that are defined by specific functional relationship with climate C (FigS. 1 S 3). The demographic rates are the survival of juveniles S_j and adults S_a, the development rate of juveniles into adults γ (maturation rate), and the fertility of adults F.

$$\mathbf{A} = \begin{bmatrix} S_j(1-\gamma) & F \\ S_j\gamma & S_a \end{bmatrix} \tag{10}$$

This model permits to simulate population dynamics of species with four contrasting life histories. Species differ in terms of reproductive strategy (semelparous vs. iteroparous), age at first reproduction (precocial vs. delayed) [Neubert & Caswell, 2000] and lifespan (short vs. long) and thus range along the slow-fast continuum of life history variation [Gaillard *et al.*, 2016] from fast species with short generation time, high reproductive output and short lifespan (species 1) to slow species with opposite characteristics (species 4) (Table 1).

We include the effects of climate acting on only one demographic parameter at a time θ_i and assume that the inter-annual variability in population growth rates is induced by climate only (i.e. $\epsilon = 0$ in eq.7). In each case, the functional relationship between demographic rates and climate $\theta_i(C)$ is either linear, sigmoid or a bell shaped curve functions (Fig 1, Fig S 3) and is defined by the equation 4 with $\epsilon = 0$ and $\beta_1 = \overline{\theta_{ih}}$ the mean demographic parameter in the historical unperturbed environment that leads to a stable population with $\overline{C} = 0$ (Table 1). Specifically, relationships can be linear functions on the real scale, with

$$\theta_i(C_t) = \beta_0 C_t + \overline{\theta_{ih}} \tag{11}$$

and results are shown only on supplementary figure S 5 for all demographic rates. Relationships can be sigmoid functions, with

$$\theta_i(C_t) == g(y = \beta_0 C_2 + \overline{\theta_{ih}}) \tag{12}$$

and g the inverse logit link function. Relationships can be bell shaped curves functions with quadratic functional relationship between demographic rate and climate:

$$\theta_i(C_t) == g(y = \beta_0 C_t^2 + \overline{\theta_{ih}}) \tag{13}$$

For most demographic rates, g is the inverse logit link function so that $\theta_i \in [0\ 1]$, but not for fertilities of species 1 to 3 that vary on the real scale.

To characterize a reasonable range of demographic rates and lifetime outcomes in the set of projected environmental conditions, β_0 vary in a specific range that depends on the functional relationship. For linear functional relationships between climate and demographic parameters (equation 11), the slope varies as: $\beta_0 \in [-0.03\ 0.03]$ (Fig. S 5). For sigmoid functional relationships the slope varies as: $\beta_0 \in [-0.15\ 0.15]$ (Fig. 3a). For bell-shaped functional relationships the slope vary as: $\beta_0 \in [-0.025\ -0.01]$ (Fig. 3b).

We calculate the time of emergence of population using the threshold methods following the same methodology as for climate (section 3). We assume that the historical population is stable in an unperturbed stationary environment with $\overline{C} = 0$ and variance σ^2; i.e. the stochastic long-run growth rate is null: $\ln(\lambda_s) = 0$ (calculated from equation 2) . $\ln(\lambda_s)$ depends on variance in annual population growth rates $\mathrm{var}(\lambda)$ [Lande *et al.*, 2003; Tuljapurkar & Orzack, 1980] that is driven by the natural climate variability σ^2 (section 2). Climate fluctuations that increase the variance of demographic rates usually decrease the stochastic long-run growth rate of populations [Engen *et al.*, 2005; Lande *et al.*, 2003; Tuljapurkar, 1982]. Hence, to set $\ln(\lambda_s) = 0$ across environmental historical conditions, the vector of demographic parameters θ is slightly tuned for each environmental variability

σ.

4.2 Time of emergence in population depends on climate variability and trend

We found that $\mathsf{ToE}_{\mathsf{pop}}$ can be predicted by the climate signal-to-noise ratio and occurs earlier as the signal-to-noise in climate becomes larger (Fig. 3). Indeed, the $\mathsf{ToE}_{\mathsf{pop}}$ is linearly and positively correlated to the $\mathsf{ToE}_{\mathsf{climate}}$ (Fig. 3) as both the variability and trend in population are positively related to the natural variability and trend of climate (Fig. 4).

Remarkably, the $\mathsf{ToE}_{\mathsf{pop}}$ can be earlier or later than the $\mathsf{ToE}_{\mathsf{climate}}$, that depends on the life history strategies and the demographic processes by which climate affects demographic rates (Fig. 3). For example, the $\mathsf{ToE}_{\mathsf{pop}}$ is earlier than $\mathsf{ToE}_{\mathsf{climate}}$ for iteroparous species when climate affects maturation or adult survival rates for long-lived species (species 3 & 4) or juvenile survival for short-lived species (species 2). Hence, some life histories may permit an earlier detection of the time at which the signal of anthropogenic climate change emerges from the noise of natural climate variability

4.3 Time of emergence in population across life histories and demographic processes

The $\mathsf{ToE}_{\mathsf{pop}}$ can be predicted by life histories and demographic processes (Fig. 3, Fig. 5). Across life histories, the $\mathsf{ToE}_{\mathsf{pop}}$ is the largest for species 1 (semelparous short-lived strategy), which have on average the largest population variations (Table 2, Fig. 5). Across demographic processes, the $\mathsf{ToE}_{\mathsf{pop}}$ is the largest for the fertility (Table 2). For iteroparous species, the $\mathsf{ToE}_{\mathsf{pop}}$ depends on the sensitivity of the population growth rate to the demographic rate affected by climate and occurs earlier as the sensitivity increases (Fig. 5). As a consequence, the $\mathsf{ToE}_{\mathsf{pop}}$ occurs later as species longevity increases when climate affects fertility and juvenile survival. However, the opposite pattern occurs when climate affects adult survival and maturation rate: $\mathsf{ToE}_{\mathsf{pop}}$ occurs earlier for long-lived than short lived species (Fig. 3, Table 2).

4.4 Time of emergence in population among different functional relationships between climate and demographic rates

Surprisingly, the type of functional relationship and its slope have little effect on the $\mathsf{ToE}_{\mathsf{pop}}$ (Fig. 3, Fig 6). Despite that the variability of the population in the historical environment is smaller for bell shape than linear relationships on the logit scale (see eq 9 section 2), both the trend and variability are larger for bell shape relationship in the non-stationary forced environment (Table 2). Indeed, the variability in the forced environment increases substantially compared to the variability in the historical environment for bell shape, while it does not change for linear relationships (Table 2). However, the ratio trend over variability is very similar between bell shape and linear relationship, and the patterns of time of emergence are very similar regardless of the shape of the functional relationship. The slope of those relationships has also little impact of the $\mathsf{ToE}_{\mathsf{pop}}$ relative to life histories and demographic processes, probably because it affects both the trend and variability simultaneously (Fig. 1).

5 Time of emergence of emperor penguin population

Emperor penguin is a relevant empirical example to test our theoretical prediction that long lived species (comparable to species 4) may permit an earlier detection of the time at which the signal of anthropogenic climate change emerges from the noise of natural climate variability (Fig. 3, section 4.2). Penguins are threatened by future climate change as most of their breeding colonies will be endangered by 2100 if greenhouse gases continue their current course [Jenouvrier *et al.*, 2020, 2014, 2021]. These declines occur through projected loss of Antarctic sea ice, which affects survival and reproduction. Adult survival is strongly affected by sea ice during four seasons of the life cycle resulting in complex non-linear bell shape relationships [Jenouvrier *et al.*, 2012]. Adult survival is maximized at intermediate levels of sea ice because neither the complete absence of sea ice (low food resources and/or high predation), nor heavy and persistent sea ice (longer foraging trip),

provide satisfactory conditions. Thus, in contrast to our theoretical examples, relationships between climate and demographic rates are even more complex for emperor penguin as sea ice affects a multitude of demographic rates during various seasons, with different functional responses among sexes, and other processes contribute to the variability in population growth rate (i.e. $\epsilon >> 0$ in eq.7, related to sampling variance and process variance due to unmeasured environment conditions such as local fast ice dynamics or large-scale atmospheric perturbations, see Trathan *et al.* [2020] for a review).

5.1 Emissions scenario, climate model and climate outputs

The climate outputs from multiple AOGCMs are publicly available in a standardized format on the Coupled Model Intercomparison Project (CMIP) website. CMIP5 provides a framework for coordinated climate change experiments for assessment in the IPCC Fifth Assessment Report (AR5) in 2014 using four Representative Concentration Pathways (RCP) describing future GHG concentration trajectories based on socio-economic assumptions. Newer emissions forcing scenarios have been developed and used for climate projections in CMIP6 for the Sixth Assessment Report (AR6) released in August 2021. These "Shared Socioeconomic Pathways" [O'Neill *et al.*, 2016](SSPs) differ in the time evolution of specific climate forcers, such as GHG and aerosol emissions, but bracket the same radiative forcing range as the RCP scenarios.

They are several sources of uncertainties in climate projections that affect the time of emergence, including the structural uncertainty associated with the different climate models used to make projections, and the scenario uncertainty associated with different future emission pathways [Deser *et al.*, 2012; Hawkins & Sutton, 2009; Schlunegger *et al.*, 2020]. However, here we use one climate model and one scenario to obtain the sea ice outputs from a large ensemble [Kay *et al.*, 2015] for illustrative purposes. In addition, large ensemble simulations using several scenarios from several climate models were not available at the time of our penguin analysis.

Specifically, we used RCP 8.5 high emission scenario [Meinshausen *et al.*, 2011], that

represents a future in which greenhouse gas emissions continue unabated. RCP 8.5 is considered as a useful scenario for quantifying physical climate risk, especially over near- to midterm policy-relevant time horizons [Schwalm *et al.*, 2020]. Indeed, the total cumulative CO2 emissions since 2005 projected under RCP8.5 by 2020 are in close agreement with historical observed total cumulative CO2 emissions [Schwalm *et al.*, 2020]. In addition, the total cumulative CO2 emissions since 2005 projected under RCP8.5 by 2050 agree well with energy forecasts under current and stated policies by 2050, with still highly plausible levels of CO2 emissions by 2100 [Schwalm *et al.*, 2020].

We use sea ice outputs from a large ensemble produced by a General Circulation Models: the community Earth System Model (CESM), developed by the National Center for Atmospheric Research (NCAR) allowing us to characterize the natural climate variability [Kay *et al.*, 2015]. In addition, CESM model resolves very well the Antarctic sea ice conditions that influence the most emperor penguin population growth rates [Jenouvrier *et al.*, 2020].

5.2 Sea ice and penguin projections

We calculate $\mathsf{ToE}_{\mathsf{pop}}$ for the 54 known colonies around the coast of Antarctica ([Fretwell *et al.*, 2012; Fretwell & Trathan, 2009], Fig. S 8) following the approach outlined in section 3 based on projections of population growth rates driven by sea ice changes. Specifically, to project emperor penguin population growth rate at each colony, we link a climate-dependent demographic matrix model to sea ice projections (section 5.1). Our sea ice-dependent demographic model includes demographic rates that depend on the sea ice conditions during four seasons (non-breeding, laying, incubating and rearing), and accounts for differences in the impact of sea ice conditions on adult survival between sexes. These relationships and their estimations are described in detail in Jenouvrier *et al.* [2012]. The model includes sources of stochasticity and uncertainties: (1) parameter uncertainty describes statistical uncertainty in the estimates of demographic parameters (e.g., survival, and their responses to sea ice concentration anomalies) and (2) process variance

(i.e., environmental stochasticity) reflects true "unexplained" temporal variance in demographic rates that is not accounted for by sea ice, which combined reflect the term $\mathrm{var}(\epsilon)$ in eq.7, section 2. As we ignored these context specific uncertainties in our theoretical simulation, we present the results with two scenario: with or without $\mathrm{var}(\epsilon)$.

For our historical environment we used sea ice projections from 1920-1950, and for the forced environment we used sea ice projections from 1950-2100 under climate scenario RCP 8.5 (section 5.1). We assume that the population is stable in the historical, unperturbed environment and our emergence threshold are based on the 90% prediction interval. This permit us to characterize when anthropogenic signals in emperor penguin populations are *very likely* to emerge from stochastic noise.

5.3 Time of emergence in sea ice and penguin

The $\mathrm{ToE}_{\mathrm{climate}}$ in sea ice varies among seasons and colonies (Fig. 7, Fig. S 6) and as a consequence, the $\mathrm{ToE}_{\mathrm{pop}}$ varies among colonies. The ToE in sea ice and populations are earlier for colonies in East Antarctica, than in the Ross, Bellinghausen, Amundsen and Wedell seas (Fig. S 8). The variability and trend are negatively related (Fig. S 7), so regions showing a larger signal also exhibit larger variability in climate and population as sea ice loss are projected into the future. When the environmental stochasticity generated by other factors than sea ice ($\mathrm{var}(\epsilon)$) is ignored, the $\mathrm{ToE}_{\mathrm{pop}}$ occurs earlier than climate for most colonies, except the ones located from Enderby Land to Terre Adelie Land in East Antarctica for which the ToE in sea ice is the earliest. When parameter uncertainty and process variance are included, the $\mathrm{ToE}_{\mathrm{pop}}$ occurs later than $\mathrm{ToE}_{\mathrm{climate}}$ for almost all colonies, except the few colonies in the Bellinghausen and Amundsen seas for sea ice during the rearing season.

6 Discussion

Anthropogenic climate change has triggered impacts on ecosystems world-wide, yet the formal timing at which these biological impacts can be detected has been insufficiently

described [Beaumont *et al.*, 2011]. Here we focused on detecting climate-driven signals in population but this approach can be applied to climate-related impacts in changes in distribution by accounting for the temporal dynamics in those spatial changes. Heretofore, changes in distribution are often assumed to depend only on the climate signal and analyses using e.g. species distribution models often ignore climate variability (but see Zimmermann *et al.* [2009]).

We found that the time of emergence of climate-driven signals in population dynamics $\mathsf{ToE}_{\mathsf{pop}}$ depends on (1) the magnitude of climate change and variability and (2) life-histories and demographic processes by which climate affects the population and we propose six testable predictions. In the context of detection and attribution of climate change, we find that some life histories magnify signal-to-noise ratios in climate ($\mathsf{ToE}_{\mathsf{climate}}$), enabling observations of populations to yield earlier detection of anthropogenic climate change than observations of a climate variable itself— while other demographic dynamics prolong the detection of anthropogenic climate change relative to $\mathsf{ToE}_{\mathsf{climate}}$.

In our emperor penguin example, frequency dependent processes occurs because of sex-biased mortality in responses to sea ice, this latter showing spatiotemporal autocorrelation, affecting reproduction and survival, resulting in complex co-variations among demographic rates, and the life cycle is structured in several stages. Our main theoretical result – some life histories enable an earlier $\mathsf{ToE}_{\mathsf{pop}}$ than $\mathsf{ToE}_{\mathsf{climate}}$– is well supported by our example when the noise is driven by climate natural variability and all complexities arising in natural systems discussed in the following sections are included.

However, when stochastic variations from observation error and other biotic and abiotic processes variability other that sea ice natural variability are included, the $\mathsf{ToE}_{\mathsf{pop}}$ occurs later than $\mathsf{ToE}_{\mathsf{climate}}$ for almost all colonies. Notwithstanding, sampling and process errors can be reduced by increasing monitoring effort and improving our understanding of how the biological systems respond to biotic and abiotic factors. In addition, aggregating abundance across space attenuates the random component of the underlying growth

rates and may permit a better detection of anthropogenic signals in populations [Che-Castaldo *et al.*, 2017].

Regardless if the stochastic noise associated with other sources than natural variability in climate occludes an earlier $\mathsf{ToE}_{\mathsf{pop}}$ than $\mathsf{ToE}_{\mathsf{climate}}$, the time of emergence identifies when the signal of anthropogenic climate change in populations can be quantitatively distinguished from year-specific stochastic variation. Quantifying $\mathsf{ToE}_{\mathsf{pop}}$ is critically needed to provide relevant cost/benefit evaluations for climate mitigation and adaptation strategies, as well as accurate assessments of the risks climate change poses to conservation and management of ecosystems [Hawkins *et al.*, 2020; Hawkins & Sutton, 2012]. Finally, we propose a road map for future research.

6.1 $\mathsf{ToE}_{\mathsf{pop}}$ is predicted from $\mathsf{ToE}_{\mathsf{climate}}$

We find that the $\mathsf{ToE}_{\mathsf{pop}}$ depends almost linearly on the $\mathsf{ToE}_{\mathsf{climate}}$ (Fig. 3). Hence, we suggest the following hypotheses.

[H1] Tropical species may permit an earlier detection of anthropogenic climate change than temperate species, especially if temperature in summer affects their demographic rates. Many climate studies have shown that the ToE in temperature is earlier for low latitude regions than for mid-latitude regions and is of intermediate duration for polar regions [Hawkins *et al.*, 2020; Hawkins & Sutton, 2012; Mahlstein *et al.*, 2012, 2011]. The emergence of signal of anthropogenic climate warming occurs the soonest in the summer season at low latitudes [Mahlstein *et al.*, 2011]. The studies of Beaumont *et al.* [2011] and Sorte *et al.* [2019] support this hypothesis: tropical and subtropical ecosystems, and mangroves, face extreme conditions earliest than boreal forests and tundra biomes because the low SD compensate for the relatively small absolute changes [Beaumont *et al.*, 2011]. Passerine bird species that migrate between temperate breeding grounds in North America and southern tropical wintering grounds experience an earlier $\mathsf{ToE}_{\mathsf{climate}}$ than species wintering in the subtropics [Sorte *et al.*, 2019]. $\mathsf{ToE}_{\mathsf{climate}}$ exceeding 2300 occurred only in the northern latitudes corresponding to the southern non-breeding grounds of some birds [Sorte *et al.*,

2019]. Studies on the thermal tolerance of terrestrial ectotherms also support this hypothesis. For example, tropical insects are relatively sensitive to temperature change and are currently living very close to their optimal temperature, while species at higher latitudes have broader thermal tolerance and are living in climates that are currently cooler than their physiological optima [Deutsch *et al.*, 2008].

[H2] In terrestrial systems, species affected by temperature may yield earlier detection of anthropogenic climate change than species affected by precipitation. Climate studies have shown that changes in precipitation are often harder to detect because natural variability in precipitation is larger than in temperature [Giorgi & Bi, 2009]. For example, the $\mathsf{ToE}_{\mathsf{climate}}$ in precipitation extremes does not occur prior to 2100 in many regions [King *et al.*, 2015]. However, an anthropogenic signal is emerging soon in wintertime heavy precipitation events over much of Eurasia and North America, so species in these regions may experience earlier $\mathsf{ToE}_{\mathsf{pop}}$. However, this hypothesis depends also on the sensitivity of the population growth rate to temperature versus precipitation. In a comparative study of time series of 165 plants populations around the globe, Compagnoni *et al.* [2021] found that demographic responses to climate are larger for precipitation than temperature, but large noise hampers the detection of the impact of precipitation on plant populations.

[H3] In marine systems, species dependent on the upper ocean biological cycling of carbon, photosynthetic activity, or salinity may yield later detection of anthropogenic climate change than species affected by sea surface temperature or PH. Several studies found that variables integrating the effect of invading anthropogenic carbon into the global ocean (e.g. pH) and sea surface temperature emerged most rapidly while variables related to the upper ocean mixing, associated changes in biological processes (e.g. export of organic matter, primary productivity) and salinity, only emerge after several decades [Henson *et al.*, 2017; Schlunegger *et al.*, 2020].

6.2 ToE in population is predicted from life histories and demographic processes

[H4] $\mathsf{ToE}_{\mathsf{pop}}$ *occurs later in selmeparous species.* Semelparous species, such as salmon, bamboos, and monocarpic herbs, exhibit a "big-bang reproduction" whereby individuals die immediately after the first reproduction [e.g. Metcalf *et al.*, 2003]. As a consequence, their population dynamics is often more variable than population of iteroparous species. Indeed, the various reproductive events of iteroparous species may be spread out throughout their life as a bet-hedging strategy in unpredictable environments, buffering the effect of environmental variability on population growth rate [Hilde *et al.*, 2020]. However, there is little theory available to predict how the degree of iteroparity might influence the demographic response to climate. A comparative study found no correlation between the degree of iteroparity with population responses to climate in plants [Compagnoni *et al.*, 2021]. Further work should entail a direct comparison of the influence of the generation time and degree of iteroparity on $\mathsf{ToE}_{\mathsf{pop}}$.

[H5] The $\mathsf{ToE}_{\mathsf{pop}}$ *of iteropareous species depends on the sensitivity of the population growth rate to the demographic parameter affected by climate* (Fig. 5). For population dynamics that are mainly affected by the impact of climate on adult survival during the non-breeding season ('tub' hypothesis, Sæther *et al.* [2004]), the $\mathsf{ToE}_{\mathsf{pop}}$ will occurs earlier in long lived species than short lived species. This might be the case for many migratory species, when the climate conditions affects survival during the migration, and in the non breeding quarters [Sorte *et al.*, 2019]. The 'tap' hypothesis [Sæther *et al.*, 2004] proposes that environmental conditions during the breeding season affect population size the following year because it influences the inflow of new recruits into the population. The $\mathsf{ToE}_{\mathsf{pop}}$ in population occurs earlier if climate conditions during the breeding season have carry-over effect on demographic rates influencing the number of recruits, as observed in many species [e.g. Szostek & Becker, 2015]. Specifically, this will occur when climate affects juvenile survival for short lived species and maturation rate for long lived species. Obviously, the underlying processes of the 'tub- tap' effects are not mutually exclusive, and

multiple demographic rates are affected by climate, that will eventually shorten or prolong the $\mathsf{ToE}_{\mathsf{pop}}$.

[H6] Iteropareous species can act as earlier indicators of the detection of anthropogenic climate change than climate itself. Earlier $\mathsf{ToE}_{\mathsf{pop}}$ than $\mathsf{ToE}_{\mathsf{climate}}$ occurs when climate affects the demographic rates that most influence the population growth rate: adult survival and maturity for long-lived iteroparous species and juvenile survival for short-lived ones (Fig. 3, Fig. 5). This hypothesis is supported by our empirical example: the population growth rate is mostly sensitive to the adult survival [Jenouvrier *et al.*, 2010], which is affected by sea ice conditions [Jenouvrier *et al.*, 2012]. Here, we found that the $\mathsf{ToE}_{\mathsf{pop}}$ occurs earlier than $\mathsf{ToE}_{\mathsf{climate}}$ when process variance due to other environmental factors and demographic parameter uncertainties is ignored (Fig. 7a). In natural system, the process variance may be large, obscuring an earlier detection of anthropogenic climate change in populations than in climate variables itself (Fig. 7b, Sæther *et al.* [2007, 2004]). However, if the goal is to use earlier indicator species in the detection of anthropogenic climate change, it is possible to reduce the demographic parameter uncertainties with higher sampling effort and decrease the process variance by a better understanding of the factors affecting the demographic processes.

6.3 Road map for the future

We provide the first theoretical study of the $\mathsf{ToE}_{\mathsf{pop}}$ to understand the proximate mechanisms of the impact of climate change and variability and demographic processes using a simple model. We illustrate how to use a climate explicit population model to quantify $\mathsf{ToE}_{\mathsf{pop}}$ for emperor penguin, and argue that climate-dependent demographic models could be developed for several species allowing future comparative analysis. But many questions remained unanswered about the effect of more complex climate-driven demographic processes occurring in natural systems such as density-dependence, autocorrelation in climate, co-variation among demographic rates, population structure, and multiple climate drivers, to name a few. We propose a road map for future research, and

acknowledge that we only scratched the surface on these important topics.

6.3.1 Comparative studies of the ToE in population using climate explicit population models

Characterizing the time of emergence requires long-term time series to define the historical unperturbed state. For many species, the unperturbed state benchmark is not available as most long-term ecological times series cover only recent decades while profound global changes were already underway. It is challenging to characterize ToE from observations in natural systems using statistical approaches, even in climate sciences. Hence, most the climate studies have used climate outputs from atmospheric–oceanic global circulation models (AOGCMs) to quantify the $\mathsf{ToE}_{\mathsf{climate}}$ [Hawkins *et al.*, 2020; Hawkins & Sutton, 2012]. Similarly, we propose to develop climate explicit population models to characterize the ToE in population. We have illustrated our approach using a simple structured population matrix model [Caswell, 2001], but other demographic, trait-based or eco-evolutionary modeling frameworks can be developed.

We argue that the $\mathsf{ToE}_{\mathsf{pop}}$ can be quantified for many species already [Doak & Morris, 2010; Saether *et al.*, 2019; Treurnicht *et al.*, 2016] allowing comparative studies to address our specific hypotheses on the variations of $\mathsf{ToE}_{\mathsf{pop}}$ across regions, ecosystems drivers, and species life histories. In recent decades, there in an increase in the number of studies measuring the effect of climate accounting for multiple seasonal and carry-over effects of climate on the complete life cycle of a species [Cordes *et al.*, 2020; Doak & Morris, 2010; Iles & Jenouvrier, 2019; Jenouvrier, 2013; Ozgul *et al.*, 2010]. Although fewer studies have developed climate-dependent population model, the information is available in the literature to integrate the statistical relationships between climate and demographic rates into population models. The last step requires an interdisciplinary approach to use climate-dependent population models with projections of historical and future climate from AOGCMs [Iles & Jenouvrier, 2019; Jenouvrier, 2013]. AOGCMs project (often non-linear) changes in climate over time, and critically, provide quantitative estimates of nat-

ural climate variability [Kay *et al.*, 2015]. We hope that ecologists will take advantage of the free availability of climate outputs in both the pre-industrial, historical and future environment supervised by the Coupled Model Intercomparison Project (section 5.1). The most recently completed phase of the project (CMIP6) includes more climate models and output variables than previous phases, and importantly, includes several large ensemble runs of the same AOGCMs and experiment to account for natural variability in climate models [Deser *et al.*, 2020].

Finally, the key to quantify the $\mathsf{ToE}_{\mathsf{pop}}$ is to characterize the population variability in the historical stationary environment. This requires careful consideration of the demographic stochasticity, especially for small populations, environmental stochasticity not driven by climate, density-dependence and interactions with other species, which can be incorporated in demographic models [Lande *et al.*, 2003].

6.3.2 Density-dependence

Our population model does not include density dependence. The impact on the $\mathsf{ToE}_{\mathsf{pop}}$ will depend on the strength and type of the density dependence (negative density dependence: exact compensation, over-compensation, under-compensation, positive density dependence), the specific demographic rate that is affected by density dependence, the interaction between climate and density dependence and the life history of the species. For example, populations with undercompensating growth tend to respond slowly to environmental changes [Gamelon *et al.*, 2017; Hansen *et al.*, 2019], that may prolongs the $\mathsf{ToE}_{\mathsf{pop}}$. For population declining in response to climate change the results should be qualitatively similar, except if Allee effects occur (a positive relationship between demographic rates and population), thereby accelerating extinction rate at low density [Courchamp *et al.*, 2008, 1999]. Allee effect will increase the magnitude of the decline of the population trend and $\mathsf{ToE}_{\mathsf{pop}}$ will probably occurs earlier [Lande, 1998], but that will depend if an increase variance compensate for this larger signal. For population increasing in response to climate change, the patterns found without density dependence are more likely

to change, that will depend on the emergence thresholds and carrying capacity of the population. For example, for invasive species, the emergence thresholds may be defined well below the carrying capacity of the population, hence the results would be qualitatively the same as without density dependence. However, if the emergence thresholds are defined above the carrying capacity, the signal of anthropogenic climate change in population cannot be formally distinguished from population variability.

6.3.3 Temporal autocorrelation in climate and demographic rates

Our simulated environment does not include autocorrelation in the climate time series, while most environmental variables exhibit a red noise that may increase the probability of extinction of populations [Mustin *et al.*, 2013; Rescan *et al.*, 2020]. Environmental variables in reddened environments imply consecutive periods of favourable or unfavourable conditions (positive autocorrelation), and a lower probability of at least one extremely poor year compared with white noise for a given time period, which may both decrease or increase population extinction risk [Schwager *et al.*, 2006]. The response of species to coloured environmental variations depends on the time-scale considered, the strength of environmental fluctuations, the particular life-history traits that are affected by environmental change and the species life cycle defining the sensitivity of population dynamics to these fluctuations [Engen *et al.*, 2013]. For example, a study from 454 plant and animal populations found that fast life histories show highest sensitivities to temporal autocorrelation in demographic rates across reproductive strategies, while slow life histories are less sensitive to temporal autocorrelation, but their sensitivities increase for species with a large degree of iteroparity [Paniw *et al.*, 2017]. An important question is then how the sensitivities to temporal autocorrelation in demographic rates is related to the $\mathsf{ToE}_{\mathsf{pop}}$, and can be addressed by incorporating such autocorrelation in our current framework. Since the patterns of the sensitivities of the population growth rate to both interannual variability and temporal autocorrelation in demographic rates are similar [Iles *et al.*, 2019; Paniw *et al.*, 2017], and the influence of autocorrelations on the population

variability driven by environmental noise is small [Engen *et al.*, 2013], we do not expect that including temporal autocorrelation will change our six hypothesis.

6.3.4 Correlation among demographic rates

Correlations among demographic rates can occur when climate affects rates simultaneously, and were ignored in our simulations. Positive covariation and autocorrelation in demographic rates tend to increase the variability in demographic rates, decreasing the stochastic growth rate and increasing the variability in population growth rates [Engen *et al.*, 2013; Tuljapurkar *et al.*, 2009]. On the opposite, negative covariation and autocorrelation tends to decrease the variability in demographic rates, such as the survival-fecundity-trade-offs that reduces the variance in the population growth rate [Colchero *et al.*, 2019; Sæther & Engen, 2015]. Correlations of opposite signs among the various demographic rates may cancel out the effect of each other, and the resulting effect on the population growth rate maybe small. In addition, the life-history strategy and density dependence affect the population responses to covariation and autocorrelation in demographic rates [Colchero *et al.*, 2019; Iles *et al.*, 2019] making challenging to predict how the trend and variability in population, hence the $\mathsf{ToE}_{\mathsf{pop}}$, will be affected by covariation among demographic rates. Demographic rate correlations had the largest effect on the population growth rate for life histories with short to medium generation time [Iles *et al.*, 2019], that may amplify or dampen the detection of anthropogenic climate change.

6.3.5 Population structure

Our population model includes the simplest age-structure by aggregating age-classes into two stages: juvenile and adult. Although this simple life cycle is useful to explore a wide range of life histories (Table 1), it leads to a reduced variance in annual population growth rates in an unperturbed environment [Colchero *et al.*, 2019]. In our definition, the $\mathsf{ToE}_{\mathsf{pop}}$ is based on the comparison of the variability between the unperturbed and perturbed environment. Hence, the resulting $\mathsf{ToE}_{\mathsf{pop}}$ should not be highly sensible to the structure of the population, except if such structure buffers or amplifies the population

variability response to population structure in a non-stationary environment. Further work focusing on how age, stage and trait structure affect the dynamics of populations and potentially dampen or amplify the climate-driven variability in population (e.g. cohort resonance, Bjørnstad *et al.* [2004]), will provide fundamental insights to theoretical and applied research of the detection of anthropogenic climate change. For example, Bjørnstad *et al.* [2004] showed that spectral frequencies of the catches of cod in the Skagerrak were not the dominant frequencies of key environmental drivers, rather there was a spectral shift with a frequency peak at cod generational time scales, the so-called cohort resonance. Population dynamics may also potentially retain a memory of prior forcing, especially when climate events occurring in one season or stage of the life cycle affect individual performance in a subsequent season or stage (e.g. carry-over effects of climate; effect of climate at young age classes that may delay age at first recruitment [Hollowed & Sundby, 2014; Lindström & Kokko, 2002; Ranta *et al.*, 2005]).

6.3.6 Multiple climate drivers

Our modeling framework includes only a single environmental time series. The cumulative integrations of white-noise atmospheric forcing in ecosystems drivers can generate population responses that are characterized by strong transitions and prolonged apparent state changes in marine ecosystems that will affect the $\mathsf{ToE}_{\mathsf{pop}}$ [Di Lorenzo & Ohman, 2013]. In addition, integrating multiple drivers to characterize the $\mathsf{ToE}_{\mathsf{pop}}$ is important as different climate variables affect organisms at various seasons and stages of their life cycle, sometimes in opposite ways [Jenouvrier, 2013; Jenouvrier *et al.*, 2018]. In a butterfly species, warmer temperatures have a positive effect on the survival of eggs, prediapause larvae and pupae but a negative effect on the survival of overwintering larvae [Radchuk *et al.*, 2013]. Climatic conditions experienced at different stages cause complex patterns of environmental covariance among demographic rates even across generations, which may either buffer or amplify the signal of anthropogenic climate change, emphasizing the importance of considering the complete life history of individuals when pre-

dicting and detecting the effect of climatic change on population dynamics [Herfindal *et al.*, 2015; Iles *et al.*, 2019; Jenouvrier, 2013].

7 Conclusion

In the current global biodiversity crisis, the development of tools to detect, quantify, and compare the signal of anthropogenic climate change is essential to understand, anticipate and adapt to climate change. Here, we provide a new perspective on how climate-induced changes in populations can be detected by quantifying the Time of Emergence in populations. We hope that ecologists will embrace the relevance of this concept in their attempt to understand population responses to climate change in non-stationary environments and provide a robust assessment of future climate risk to inform management and policy decisions.

Acknowledgments

We thank all the field workers who participated to the emperor penguin long-term study since 1964, and the Institute Paul Emile Victor (Programme IPEV 109), and Terres Australes et Antarctiques Françaises for for logistical and financial support in Terre Adélie. We thank Joannie Van de Walle and Remi Fay for their comments on earlier versions of the manuscript and Arpat Ozgul, David Iles, Jimmy Garnier, Mike Neubert and the working group on "Individual heterogeneity in animal's life histories" for constructive discussions. We acknowledge the support of NASA 80NSSC20K1289 to SJ, ML and MH and NSF OPP 1744794 to SJ.

8 References

Barnes E, Anderson C, Ebert-Uphoff I (2018) An ai approach to determining the time of emergence of climate change. In: *Proc. 8th International Workshop on Climate Informatics: CI 2018*, pp. 19–22.

Barnhart KR, Miller CR, Overeem I, Kay JE (2016) Mapping the future expansion of arctic open water. *Nature Climate Change*, **6**, 280–285.

Barraquand F, Yoccoz NG (2013) When can environmental variability benefit population growth? counterintuitive effects of nonlinearities in vital rates. *Theoretical population biology*, **89**, 1–11.

Beaumont LJ, Pitman A, Perkins S, Zimmermann NE, Yoccoz NG, Thuiller W (2011) Impacts of climate change on the world's most exceptional ecoregions. *Proceedings of the National Academy of Sciences*, **108**, 2306–2311.

Bienvenu F, Legendre S (2015) A new approach to the generation time in matrix population models. *The American Naturalist*, **185**, 834–843.

Bjørnstad ON, Nisbet RM, FROMENTIN JM (2004) Trends and cohort resonant effects in age-structured populations. *Journal of animal ecology*, **73**, 1157–1167.

Boyce M, Haridas C, Lee C, Thenceasstochasticdemographyw (2006) Demography in an increasingly variable world. *Trends in Ecology & Evolution*, **21**, 141–148. doi:10.1016/j.tree.2005.11.018.

Callendar GS (1938) The artificial production of carbon dioxide and its influence on temperature. *Quarterly Journal of the Royal Meteorological Society*, **64**, 223–240.

Caswell H (2001) *Matrix population models*, vol. Second. Sinauer, Sunderland, Massachusetts, - pp.

Che-Castaldo C, Jenouvrier S, Youngflesh C, *et al.* (2017) Pan-antarctic analysis aggre-

gating spatial estimates of adélie penguin abundance reveals robust dynamics despite stochastic noise. *Nature communications*, **8**, 832.

Colchero F, Jones OR, Conde DA, *et al.* (2019) The diversity of population responses to environmental change. *Ecology Letters*. doi:10.1111/ele.13195.

Compagnoni A, Levin S, Childs DZ, *et al.* (2021) Herbaceous perennial plants with short generation time have stronger responses to climate anomalies than those with longer generation time. *Nature Communications*, **12**. doi:10.1038/s41467-021-21977-9.

Cordes LS, Blumstein DT, Armitage KB, *et al.* (2020) Contrasting effects of climate change on seasonal survival of a hibernating mammal. *Proceedings of the National Academy of Sciences*, **117**, 18119–18126.

Courchamp F, Berec L, Gascoigne J (2008) *Allee effects in ecology and conservation*. Oxford University Press.

Courchamp F, Clutton-Brock T, Grenfell B (1999) Inverse density dependence and the allee effect. *Trends in ecology & evolution*, **14**, 405–410.

Deser C, Knutti R, Solomon S, Phillips AS (2012) Communication of the role of natural variability in future north american climate. *Nature Climate Change*, **2**, 775–779.

Deser C, Lehner F, Rodgers KB, *et al.* (2020) Insights from earth system model initial-condition large ensembles and future prospects. *Nature Climate Change*, **10**, 277–286. doi:10.1038/s41558-020-0731-2.

Deutsch CA, Tewksbury JJ, Huey RB, Sheldon KS, Ghalambor CK, Haak DC, Martin PR (2008) Impacts of climate warming on terrestrial ectotherms across latitude. *Proceedings of the National Academy of Sciences*, **105**, 6668–6672. doi:10.1073/pnas.0709472105.

Di Lorenzo E, Ohman MD (2013) A double-integration hypothesis to explain ocean ecosystem response to climate forcing. *Proceedings of the National Academy of Sciences*, **110**, 2496–2499.

Doak DF, Morris WF (2010) Demographic compensation and tipping points in climate-

induced range shifts. *Nature*, **467**, 959–962.

Engen S, Bakke Ø, Islam A (1998) Demographic and environmental stochasticity-concepts and definitions. *Biometrics*, pp. 840–846.

Engen S, Lande R, Sæther BE (2013) A quantitative genetic model of r-and k-selection in a fluctuating population. *The American Naturalist*, **181**, 725–736.

Engen S, Lande R, Sæther BE, Weimerskirch H (2005) Extinction in relation to demographic and environmental stochasticity in age-structured models. *Mathematical biosciences*, **195**, 210–227.

Fretwell PT, LaRue MA, Morin P, *et al.* (2012) An Emperor Penguin Population Estimate: The First Global, Synoptic Survey of a Species from Space. *PLoS ONE*, **7**, e33751.

Fretwell PT, Trathan PN (2009) Penguins from space: faecal stains reveal the location of emperor penguin colonies. *Global Ecology and Biogeography*, **18**, 543–552. doi:10.1111/j.1466-8238.2009.00467.x.

Gaillard J, Yoccoz N (2003) Temporal variation in survival of mammals: a case of environmental canalization? *Ecology*, **84**, 3294–3306.

Gaillard JM, Lemaître JF, Berger V, *et al.* (2016) *Encyclopedia of Evolutionary Biology.*, chap. Life Histories, Axes of Variation, p. 312–323. Oxford: Academic Press.

Gaillard JM, Mark Hewison A, Klein F, Plard F, Douhard M, Davison R, Bonenfant C (2013) How does climate change influence demographic processes of widespread species? lessons from the comparative analysis of contrasted populations of roe deer. *Ecology letters*, **16**, 48–57.

Gamelon M, Grøtan V, Nilsson AL, *et al.* (2017) Interactions between demography and environmental effects are important determinants of population dynamics. *Science Advances*, **3**, e1602298.

Ghil M (2002) Natural climate variability. *Encyclopedia of global environmental change*, **1**, 544–549.

Giorgi F, Bi X (2009) Time of emergence (TOE) of GHG-forced precipitation change hotspots. *Geophysical Research Letters*, **36**. doi:10.1029/2009gl037593.

Hansen BB, Gamelon M, Albon SD, *et al.* (2019) More frequent extreme climate events stabilize reindeer population dynamics. *Nature communications*, **10**, 1–8.

Hawkins E, Frame D, Harrington L, Joshi M, King A, Rojas M, Sutton R (2020) Observed emergence of the climate change signal: From the familiar to the unknown. *Geophysical Research Letters*, **47**. doi:10.1029/2019gl086259.

Hawkins E, Sutton R (2009) The potential to narrow uncertainty in regional climate predictions. *Bulletin of the American Meteorological Society*, **90**, 1095–1108.

Hawkins E, Sutton R (2012) Time of emergence of climate signals. *Geophysical Research Letters*, **39**, n/a–n/a. doi:10.1029/2011gl050087.

Henson SA, Beaulieu C, Ilyina T, *et al.* (2017) Rapid emergence of climate change in environmental drivers of marine ecosystems. *Nature Communications*, **8**. doi:10.1038/ncomms14682.

Herfindal I, van de Pol M, Nielsen JT, Sæther BE, Møller AP (2015) Climatic conditions cause complex patterns of covariation between demographic traits in a long-lived raptor. *Journal of Animal Ecology*, **84**, 702–711.

Hilde CH, Gamelon M, Sæther BE, Gaillard JM, Yoccoz NG, Pélabon C (2020) The demographic buffering hypothesis: evidence and challenges. *Trends in ecology & evolution*, **35**, 523–538.

Hollowed AB, Sundby S (2014) Change is coming to the northern oceans. *Science*, **344**, 1084–1085.

Iles D, Jenouvrier S (2019) *Projected population consequences of climate change*, pp. 147–164. Oxford University Press.

Iles DT, Rockwell RF, Koons DN (2019) Shifting vital rate correlations alter predicted population responses to increasingly variable environments. *The American Naturalist*, **193**,

E57–E64. doi:10.1086/701043.

Jenouvrier S (2013) Impacts of climate change on avian populations. *Global Change Biology*, **19**, 2036–2057.

Jenouvrier S, Caswell H, Barbraud C, Weimerskirch H (2010) Mating behavior, population growth, and the operational sex ratio: A periodic two-sex model approach. *The American naturalist*, **175**, 739–752. doi:10.1086/652436.

Jenouvrier S, Desprez M, Fay R, Barbraud C, Weimerskirch H, Delord K, Caswell H (2018) Climate change and functional traits affect population dynamics of a long-lived seabird. *Journal of Animal Ecology*, **87**, 906–920.

Jenouvrier S, Holland M, Iles D, *et al.* (2020) The paris agreement objectives will likely halt future declines of emperor penguins. *Global change biology*, **26**, 1170–1184.

Jenouvrier S, Holland M, Stroeve J, Barbraud C, Weimerskirch H, Serreze M, Caswell H (2012) Effects of climate change on an emperor penguin population: analysis of coupled demographic and climate models. *Global Change Biology*, **18**, 2756–2770. doi:10.1111/j.1365-2486.2012.02744.x.

Jenouvrier S, Holland M, Stroeve J, Serreze M, Barbraud C, Weimerskirch H, Caswell H (2014) Projected continent-wide declines of the emperor penguin under climate change. *Nature Climate Change*, **4**, 715.

Jenouvrier S, Judy CC, Wolf S, *et al.* (2021) The call of the emperor penguin: Legal responses to species threatened by climate change. *Global Change Biology*.

Kay J, Deser C, Phillips A, *et al.* (2015) The community earth system model (cesm) large ensemble project: A community resource for studying climate change in the presence of internal climate variability. *Bulletin of the American Meteorological Society*, **96**, 1333–1349.

King AD, Donat MG, Fischer EM, *et al.* (2015) The timing of anthropogenic emergence in simulated climate extremes. *Environmental Research Letters*, **10**, 094015.

Lande R (1998) Anthropogenic, ecological and genetic factors in extinction and conserva-

tion. *Population Ecology*, **40**, 259–269.

Lande R, Engen S, Saether B (2003) *Stochastic Population Dynamics in Ecology and Conservation.* Oxford University Press.

Landrum L, Holland MM (2020) Extremes become routine in an emerging new arctic. *Nature Climate Change*, **10**, 1108–1115.

Lindström J, Kokko H (2002) Cohort effects and population dynamics. *Ecology Letters*, **5**, 338–344.

Lyu K, Zhang X, Church JA, Slangen AB, Hu J (2014) Time of emergence for regional sea-level change. *Nature Climate Change*, **4**, 1006–1010.

Mahlstein I, Daniel JS, Solomon S (2013) Pace of shifts in climate regions increases with global temperature. *Nature Climate Change*, **3**, 739–743. doi:10.1038/nclimate1876.

Mahlstein I, Hegerl G, Solomon S (2012) Emerging local warming signals in observational data. *Geophysical Research Letters*, **39**, n/a–n/a. doi:10.1029/2012gl053952.

Mahlstein I, Knutti R, Solomon S, Portmann RW (2011) Early onset of significant local warming in low latitude countries. *Environmental Research Letters*, **6**, 034009.

Mann ME, Steinman BA, Brouillette DJ, Miller SK (2021) Multidecadal climate oscillations during the past millennium driven by volcanic forcing. *Science*, **371**, 1014–1019.

Mason LR, Green RE, Howard C, *et al.* (2019) Population responses of bird populations to climate change on two continents vary with species' ecological traits but not with direction of change in climate suitability. *Climatic Change*, **157**, 337–354. doi:10.1007/s10584-019-02549-9.

Meinshausen M, Smith SJ, Calvin K, *et al.* (2011) The rcp greenhouse gas concentrations and their extensions from 1765 to 2300. *Climatic change*, **109**, 213–241.

Metcalf JC, Rose KE, Rees M (2003) Evolutionary demography of monocarpic perennials. *Trends in Ecology & Evolution*, **18**, 471–480.

Mora C, Frazier AG, Longman RJ, *et al.* (2013) The projected timing of climate departure

from recent variability. *Nature*, **502**, 183–187.

Morris W, Pfister C, Tuljapurkar S, *et al.* (2008) Longevity can buffer plant and animal populations against changing climate variability. *ecology*, **89**, 19–25.

Mustin K, Dytham C, Benton TG, Travis JMJ (2013) Red noise increases extinction risk during rapid climate change. *Diversity and Distributions*, **19**, 815–824. doi:10.1111/ddi.12038.

Neubert M, Caswell H (2000) Density-dependent vital rates and their population dynamic consequences. *J Math Biol*, **41**, 103–121.

O'Neill BC, Tebaldi C, Vuuren DPv, *et al.* (2016) The scenario model intercomparison project (scenariomip) for cmip6. *Geoscientific Model Development*, **9**, 3461–3482.

Ozgul A, Childs DZ, Oli MK, *et al.* (2010) Coupled dynamics of body mass and population growth in response to environmental change. *Nature*, **466**, 482.

Paniw M, Ozgul A, Salguero-Gómez R (2017) Interactive life-history traits predict sensitivity of plants and animals to temporal autocorrelation. *Ecology Letters*, **21**, 275–286. doi:10.1111/ele.12892.

Parmesan C, Burrows MT, Duarte CM, Poloczanska ES, Richardson AJ, Schoeman DS, Singer MC (2013) Beyond climate change attribution in conservation and ecological research. *Ecology letters*, **16**, 58–71.

Radchuk V, Turlure C, Schtickzelle N (2013) Each life stage matters: the importance of assessing the response to climate change over the complete life cycle in butterflies. *Journal of Animal Ecology*, **82**, 275–285.

Ranta E, Lundberg P, Kaitala V (2005) *Ecology of populations*. Cambridge University Press.

Rescan M, Grulois D, Ortega-Aboud E, Chevin LM (2020) Phenotypic memory drives population growth and extinction risk in a noisy environment. *Nature ecology & evolution*, **4**, 193–201.

Revelle R, Suess HE (1957) Carbon dioxide exchange between atmosphere and ocean and

the question of an increase of atmospheric co2 during the past decades. *Tellus*, **9**, 18–27.

Rojas M, Lambert F, Ramirez-Villegas J, Challinor AJ (2019) Emergence of robust precipitation changes across crop production areas in the 21st century. *Proceedings of the National Academy of Sciences*, **116**, 6673–6678. doi:10.1073/pnas.1811463116.

Román-Palacios C, Wiens JJ (2020) Recent responses to climate change reveal the drivers of species extinction and survival. *Proceedings of the National Academy of Sciences*, **117**, 4211–4217.

Roth G, Caswell H (2018) Occupancy time in sets of states for demographic models. *Theoretical Population Biology*, pp. 62–77. doi:doi:10.1016/j.tpb.2017.12.007.

Saether B, Bakke O (2000) Avian life history variation and contribution of demographic trait to the population growth rate. *Ecology*, **81**, 642–653.

Sæther BE, Engen S (2015) The concept of fitness in fluctuating environments. *Trends in ecology & evolution*, **30**, 273–281.

Saether BE, Engen S, Gamelon M, Grøtan V (2019) Predicting the effects of climate change on bird population dynamics. In: *Effects of Climate Change on Birds*, pp. 74–90. Oxford University Press.

Sæther BE, Lillegård M, Grøtan V, Filli F, Engen S (2007) Predicting fluctuations of reintroduced ibex populations: the importance of density dependence, environmental stochasticity and uncertain population estimates. *Journal of Animal Ecology*, **76**, 326–336.

Sæther BE, Sutherland WJ, Engen S (2004) Climate influences on avian population dynamics. *Advances in Ecological Research*, **35**, 185–209.

Schlunegger S, Rodgers KB, Sarmiento JL, *et al.* (2020) Time of emergence and large ensemble intercomparison for ocean biogeochemical trends. *Global Biogeochemical Cycles*, **34**. doi:10.1029/2019gb006453.

Schwager M, Johst K, Jeltsch F (2006) Does red noise increase or decrease extinction risk? single extreme events versus series of unfavorable conditions. *The American Naturalist*,

167, 879–888.

Schwalm CR, Glendon S, Duffy PB (2020) Rcp8. 5 tracks cumulative co2 emissions. *Proceedings of the National Academy of Sciences*, **117**, 19656–19657.

Sorte FAL, Fink D, Johnston A (2019) Time of emergence of novel climates for north american migratory bird populations. *Ecography*, **42**, 1079–1091. doi:10.1111/ecog.04408.

Stephens PA, Mason LR, Green RE, *et al.* (2016) Consistent response of bird populations to climate change on two continents. *Science*, **352**, 84–87.

Szostek KL, Becker PH (2015) Survival and local recruitment are driven by environmental carry-over effects from the wintering area in a migratory seabird. *Oecologia*, **178**, 643–657.

Trathan PN, Wienecke B, Barbraud C, *et al.* (2020) The emperor penguin-vulnerable to projected rates of warming and sea ice loss. *Biological Conservation*, **241**, 108216.

Treurnicht M, Pagel J, Esler KJ, *et al.* (2016) Environmental drivers of demographic variation across the global geographical range of 26 plant species. *Journal of Ecology*, **104**, 331–342. doi:10.1111/1365-2745.12508.

Tuljapurkar S, Gaillard JM, Coulson T (2009) From stochastic environments to life histories and back. *Philosophical Transactions of the Royal Society B: Biological Sciences*, **364**, 1499–1509. doi:10.1098/rstb.2009.0021.

Tuljapurkar S, Orzack S (1980) Population dynamics in variable environments I. Long-run growth rates and extinction. *Theoretical Population Biology*, **18**, 314–342.

Tuljapurkar SD (1982) Population dynamics in variable environments. iii. evolutionary dynamics of r-selection. *Theoretical population biology*, **21**, 141–165.

Vázquez DP, Gianoli E, Morris WF, Bozinovic F (2015) Ecological and evolutionary impacts of changing climatic variability. *Biological Reviews*, **92**, 22–42. doi:10.1111/brv.12216.

Zappa G, Hoskins BJ, Shepherd TG (2015) Improving climate change detection through

optimal seasonal averaging: The case of the north atlantic jet and european precipitation. *Journal of Climate*, **28**, 6381–6397.

Zimmermann NE, Yoccoz NG, Edwards TC, *et al.* (2009) Climatic extremes improve predictions of spatial patterns of tree species. *Proceedings of the National Academy of Sciences*, **106**, 19723–19728.

Figure

Figure 1: Conceptual diagram of the time of emergence (ToE) in climate ($\mathsf{ToE}_{\mathsf{climate}}$) and in populations ($\mathsf{ToE}_{\mathsf{pop}}$). ToE identifies the point in time when the signal of anthropogenic climate change (red time series) emerges from the noise associated with natural variability (black time series). $\mathsf{ToE}_{\mathsf{pop}}$ depends on the response of population growth rate to climate that is defined by: (1) the impact of climate on demographic rates (e.g. survival) with different functional forms that influence the sensitivity of demographic rates to climate; (2) the impact of demographic rates on the population growth rate resulting from non-linear demographic processes occurring throughout the species life cycle (described in section Population projections).

Figure 2:Illustrative figure of the time of emergence in climate ($\mathsf{ToE}_{\mathsf{climate}}$ on left panel) and in populations ($\mathsf{ToE}_{\mathsf{pop}}$ on right panels) of four species along the gradient of life histories, from fast species (species 1) to slow species (species 4). The figure shows one time series simulated during the historical environment (black line) and forced environment (red line). The emergence thresholds are based on a 95% prediction interval of 1000 simulations (grey area). The natural variability in climate is $\sigma = 0.5$. The forced perturbation occurs at years 80 years resulting in a positive trend in climate. Climate affects negatively maturation rate (slope of the linear relationship on logit scale: $\beta = -0.125$). Y-axis is different for each species.

Figure 3: Relationship between $\mathsf{ToE}_{\mathsf{climate}}$ (x-axis) and $\mathsf{ToE}_{\mathsf{pop}}$ (y-axis) for four life history strategies (from fast (species 1) to slow (species 4)), whereby climate affects only one demographic parameter at a time (colored dots: blue is fertility, red is juvenile survival, orange is adult survival and purple is maturation rate). Black lines represent the time when $\mathsf{ToE}_{\mathsf{pop}} = \mathsf{ToE}_{\mathsf{climate}}$.

Figure 4: a) The variability in annual population growth rates depends on the natural variability of climate σ, in both in the historical and perturbed environment (example for

$\beta = 0.125$ $\alpha = 0.05$). (b) The trend of population growth rate at the time of emergence in population depends on the trend of climate α (example for $\beta = 0.125$ and $\sigma = 0.5$). Colors refer to the climate-dependent demographic rate: blue is fertility, red is juvenile survival, orange is adult survival and purple is maturation rate. The dots on (a) stand for the forced environment while square are the historical environment. Panels show four different life history strategies, from fast (species 1) to slow (species 4).

Figure 5: $\mathsf{ToE}_{\mathsf{pop}}$ as function of the sensitivity of the population growth rate to the demographic rate affected by climate. The $\mathsf{ToE}_{\mathsf{pop}}$ is the median across various natural variability and trend of climate and various slope in the functional relationship between climate and the demographic rate (Table 1). The sensitivity of the population growth rate to the demographic rate is calculated for the averaged population matrix in the historical environment. Symbols refer to species.

Figure 6: $\mathsf{ToE}_{\mathsf{pop}}$ as function of the absolute slope of the functional relationship between climate and demographic rate β_0. Example for a climate trend of $\alpha = 0.05$ and climate variability of $\sigma = 0.5$. Colors refer to demographic pathway by which climate affects demographic rates: blue is fertility, red is juvenile survival, orange is adult survival and purple is maturation rate. The dots stand for $\beta_0 > 0$, while square shows $\beta_0 < 0$. Panels show four life history strategies.

Figure 7: Difference between the time of emergence in sea ice and $\mathsf{ToE}_{\mathsf{pop}}$ of emperor penguin ($\mathsf{ToE}_{\mathsf{climate}} - \mathsf{ToE}_{\mathsf{pop}}$) for the 54 known colonies (x-axis) and four seasons (color). The calculation of $\mathsf{ToE}_{\mathsf{pop}}$ accounts for $\mathsf{var}(\epsilon)$ generated by parameter uncertainty and process variance (i.e., environmental stochasticity) (a) or not (b).

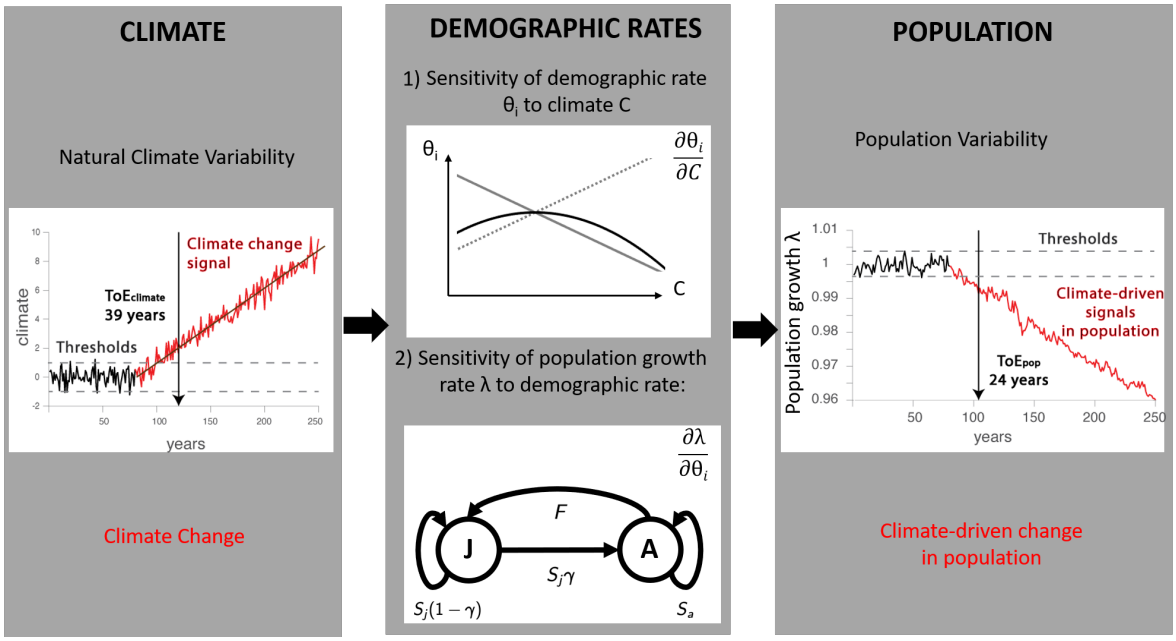

Figure 1: Conceptual diagram of the time of emergence (ToE) in climate ($ToE_{climate}$) and in populations (ToE_{pop}). ToE identifies the point in time when the signal of anthropogenic climate change (red time series) emerges from the noise associated with natural variability (black time series). ToE_{pop} depends on the response of population growth rate to climate that is defined by: (1) the impact of climate on demographic rates (e.g. survival) with different functional forms that influence the sensitivity of demographic rates to climate; (2) the impact of demographic rates on the population growth rate resulting from non-linear demographic processes occurring throughout the species life cycle (described in section Population projections).

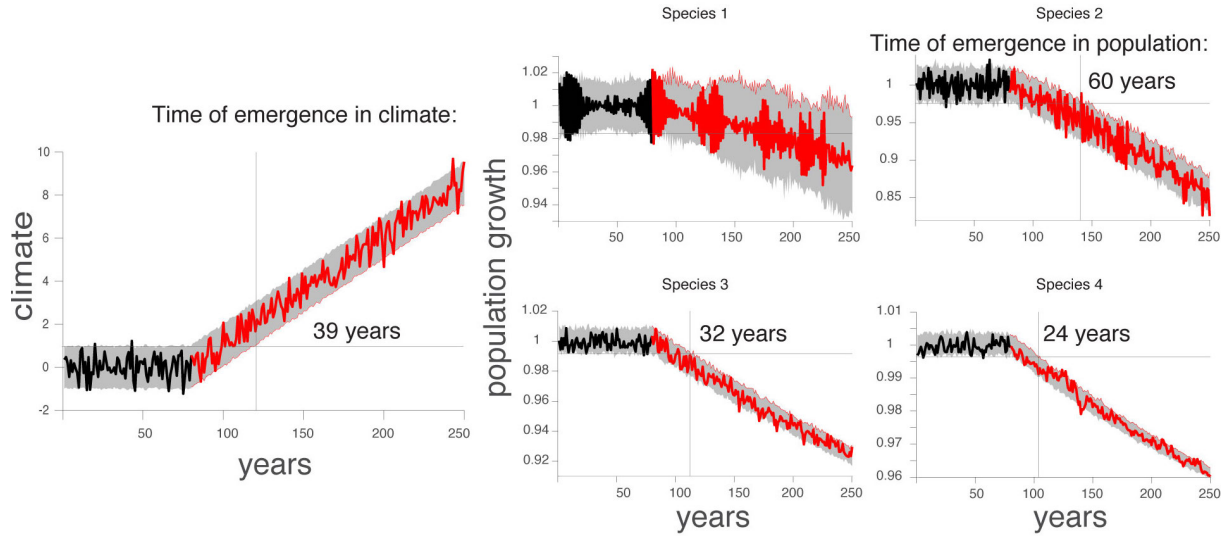

Figure 2: Illustrative figure of the time of emergence in climate ($\text{ToE}_{\text{climate}}$ on left panel) and in populations (ToE_{pop} on right panels) of four species along the gradient of life histories, from fast species (species 1) to slow species (species 4). The figure shows one time series simulated during the historical environment (black line) and forced environment (red line). The emergence thresholds are based on a 95% prediction interval of 1000 simulations (grey area). The natural variability in climate is $\sigma = 0.5$. The forced perturbation occurs at years 80 years resulting in a positive trend in climate. Climate affects negatively maturation rate (slope of the linear relationship on logit scale: $\beta = -0.125$). Y-axis is different for each species.

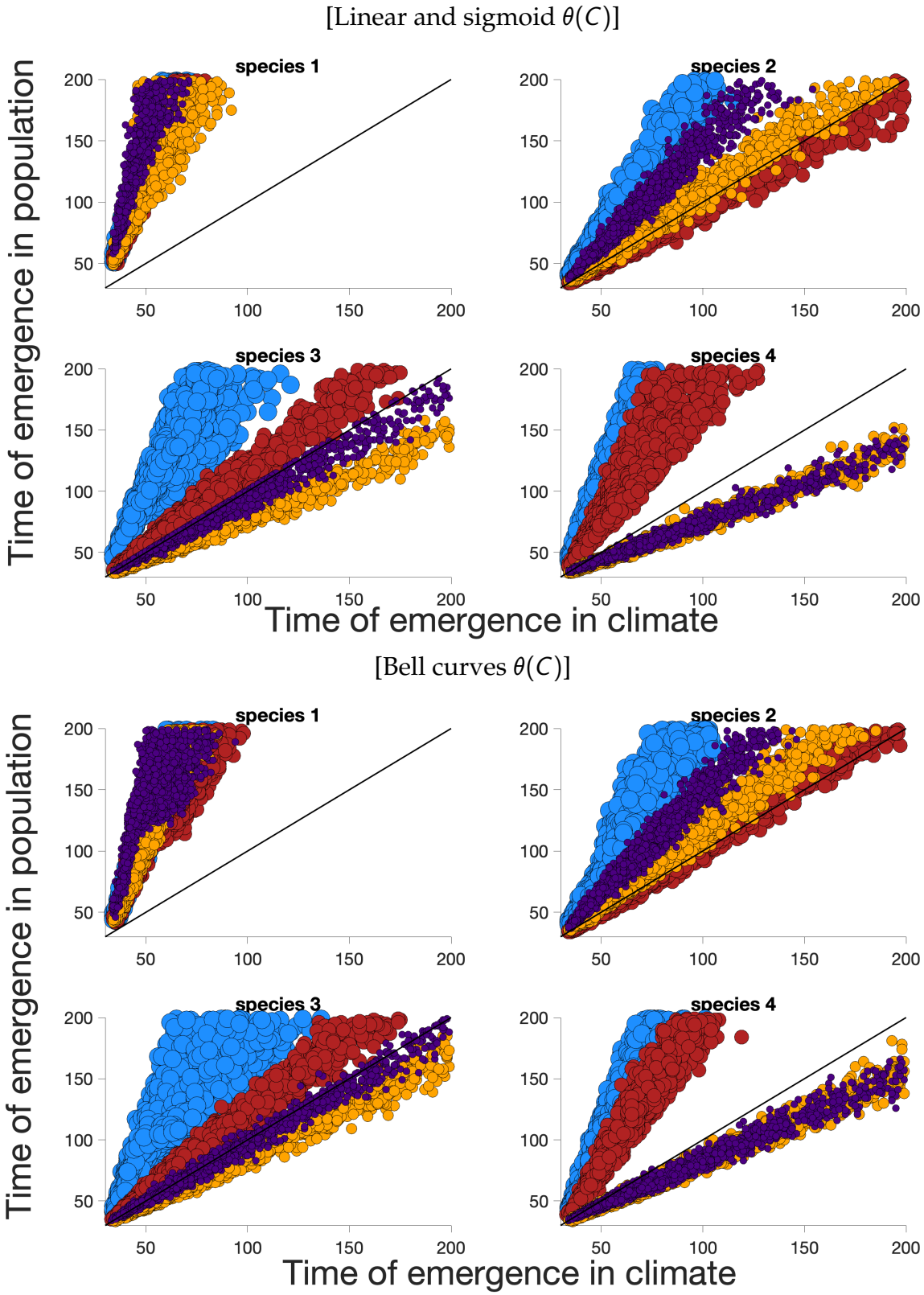

Figure 3: Relationship between $\text{ToE}_{\text{climate}}$ (x-axis) and ToE_{pop} (y-axis) for four life history strategies (from fast (species 1) to slow (species 4)), whereby climate affects only one demographic parameter at a time (colored dots: blue is fertility, red is juvenile survival, orange is adult survival and purple is maturation rate). Black lines represent the time when $\text{ToE}_{\text{pop}} = \text{ToE}_{\text{climate}}$.

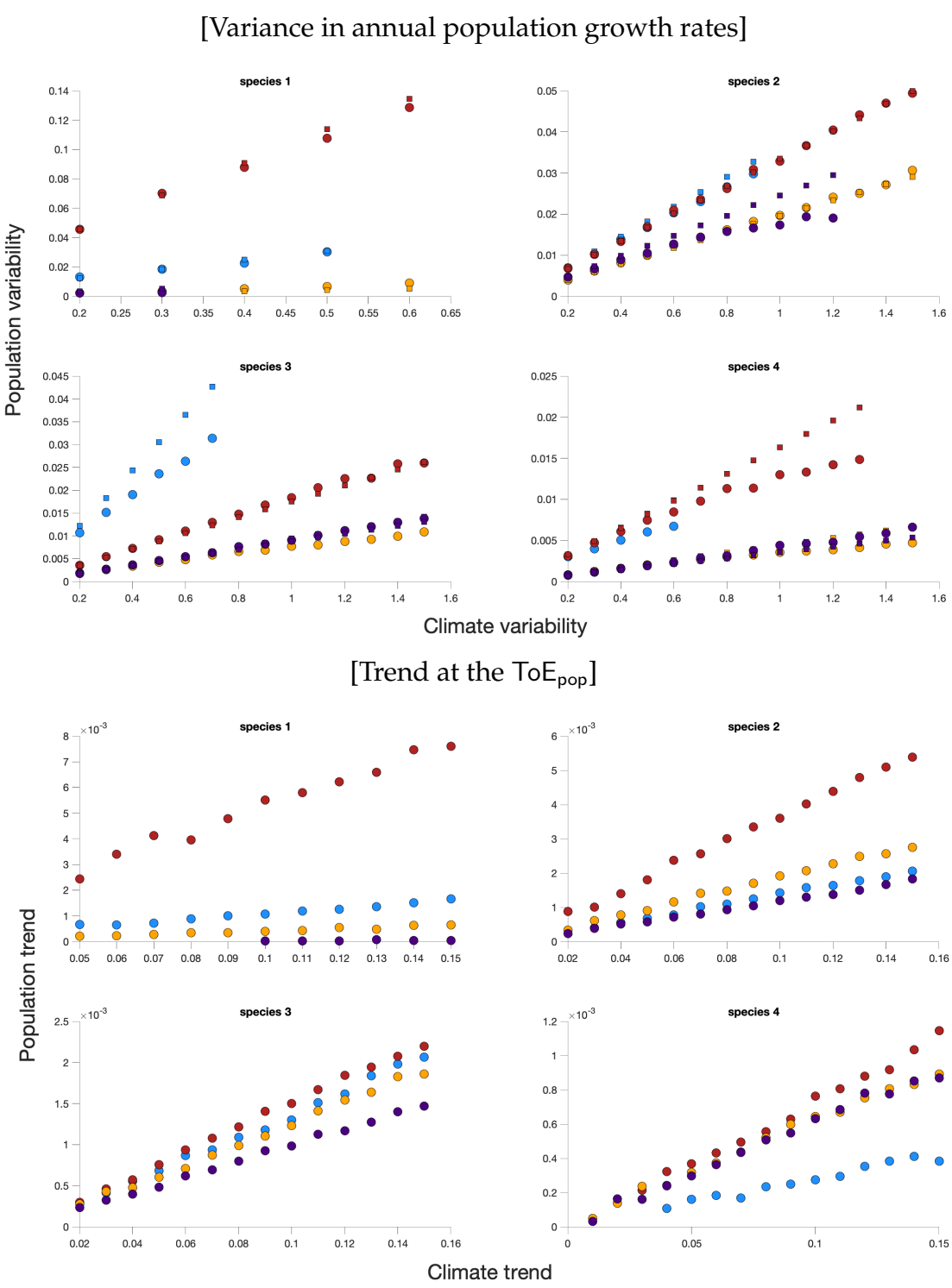

Figure 4: (a) The variability in annual population growth rates depends on the natural variability of climate σ, in both in the historical and perturbed environment (example for $\beta = 0.125$ $\alpha = 0.05$). (b) The trend of population growth rate at the time of emergence in population depends on the trend of climate α (example for $\beta = 0.125$ and $\sigma = 0.5$). Colors refer to the climate-dependent demographic rate: blue is fertility, red is juvenile survival, orange is adult survival and purple is maturation rate. The dots on (a) stand for the forced environment while square are the historical environment. Panels show four different life history strategies, from fast (species 1) to slow (species 4).

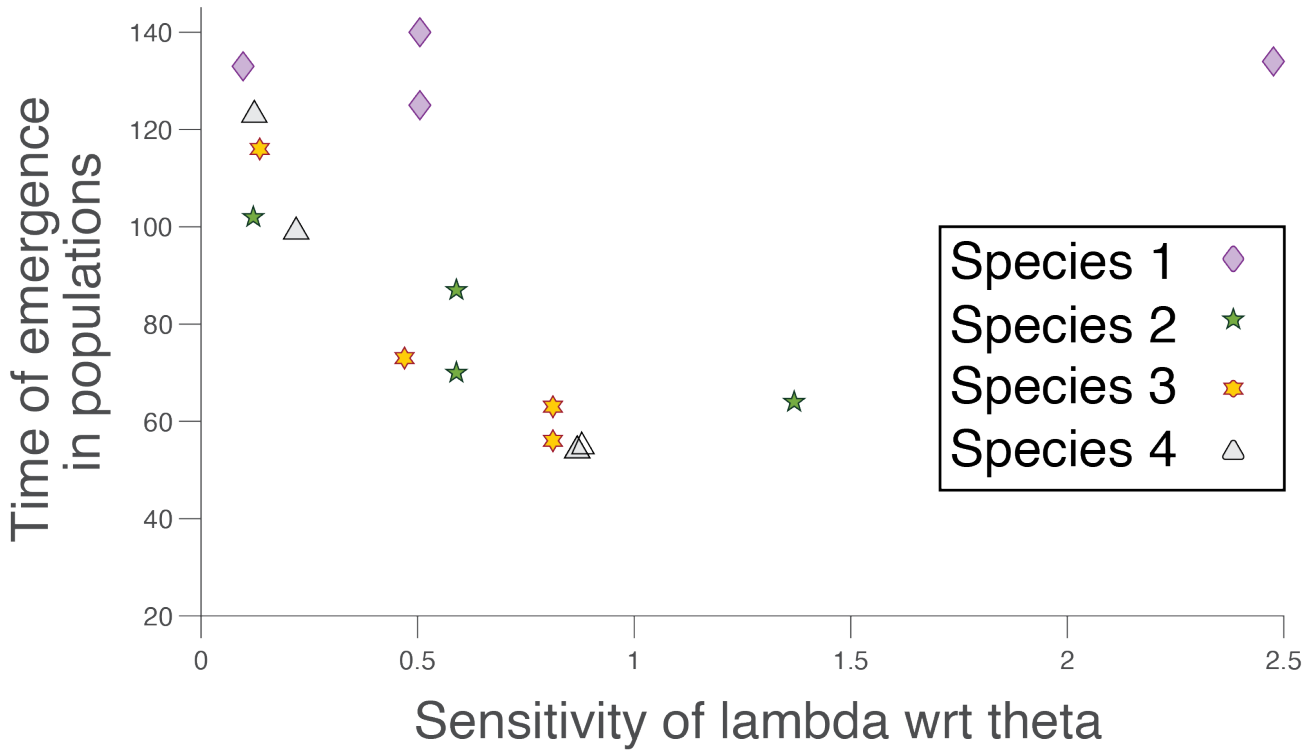

Figure 5: ToE_{pop} as function of the sensitivity of the population growth rate to the demographic rate affected by climate. The ToE_{pop} is the median across various natural variability and trend of climate and various slope in the functional relationship between climate and the demographic rate (Table 1). The sensitivity of the population growth rate to the demographic rate is calculated for the averaged population matrix in the historical environment. Symbols refer to species.

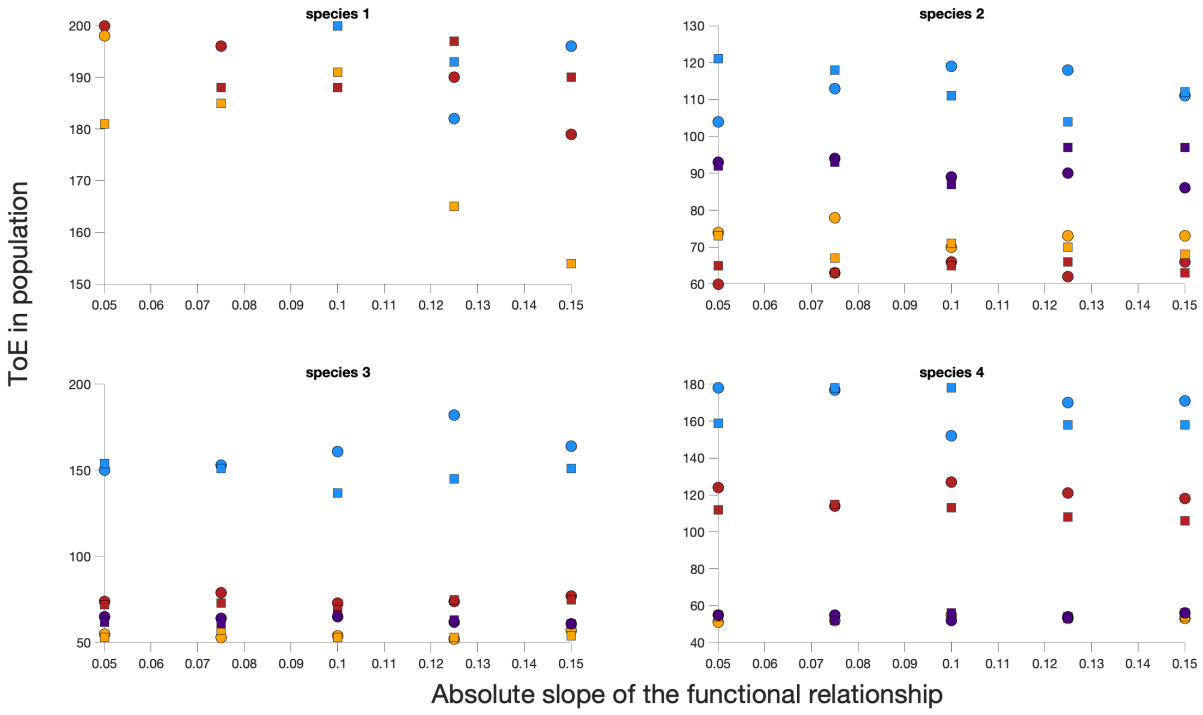

Figure 6: ToE_{pop} as function of the absolute slope of the functional relationship between climate and demographic rate β_0. Example for a climate trend of $\alpha = 0.05$ and climate variability of $\sigma = 0.5$. Colors refer to demographic pathway by which climate affects demographic rates: blue is fertility, red is juvenile survival, orange is adult survival and purple is maturation rate. The dots stand for $\beta_0 > 0$, while square shows $\beta_0 < 0$. Panels show four life history strategies.

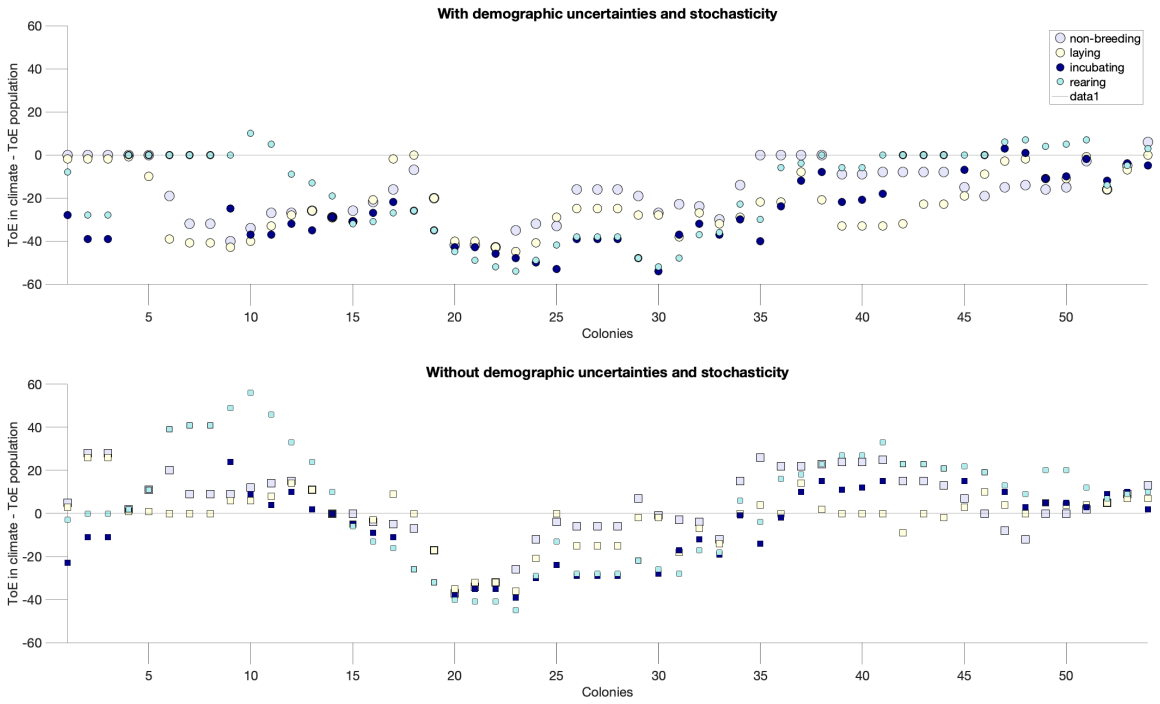

Figure 7: Difference between the time of emergence in sea ice and $\mathrm{ToE}_{\mathrm{pop}}$ of emperor penguin ($\mathrm{ToE}_{\mathrm{climate}} - \mathrm{ToE}_{\mathrm{pop}}$) for the 54 known colonies (x-axis) and four seasons (color). The calculation of $\mathrm{ToE}_{\mathrm{pop}}$ accounts for $\mathrm{var}(\epsilon)$ generated by parameter uncertainty and process variance (i.e., environmental stochasticity) (a) or not (b).

Table

Table 1: Demographic rates and outcomes for the four life history strategies (species in columns). The deterministic population growth rate is one for all species. The generation time (in years) is the mean age of parents (eq 14 of Bienvenu & Legendre [2015]), from the fundamental matrix life the following demographic outputs are calculated: the mean life expectancy at birth and the mean remaining life at adulthood (eq 20 of [Roth & Caswell, 2018]); the probability to return to the adult state (from eq 47 of [Roth & Caswell, 2018] using state A on Fig. 2). Ex stands for extreme.

	species 1	species 2	species 3	species 4
	Life history strategies			
Reproductive strategy	Semelparous	Iteroparous	Iteroparous	Iteroparous
Developmental strategy	Precocious	Precocious	Delayed	Ex-Delayed
Survival strategy	Short-lived	Short-lived	Long-lived	Ex-Long-lived
	Vital rates			
Annual fertility rate	5.06	3.00	1.00	0.50
Juvenile survival prob.	0.20	0.30	0.40	0.60
Adult survival prob.	0.03	0.39	0.83	0.93
Maturation rate	0.95	0.60	0.30	0.11
	Life history outcomes			
Generation time	2.04	2.77	7.40	16.30
Life expectancy at birth	1.21	1.47	2.39	4.17
Remaining life at adulthood	1.03	1.63	6.02	14.29
Probability to return to adult state	0.03	0.39	0.83	0.93

Table 2: Time of emergence, trend and variability of population growth rate, with its sensitivity to climate across all simulations for four life history strategies (species in row) and four demographic pathways by which climate affects demography rates (columns). Median of the time of emergence of population is denoted $\mathsf{ToE}_{\mathsf{pop}}$. At the time of emergence in the population: the median of the trend is T_{ToEpop}, the median of the variability in the forced environment is var_{ToEpop} and their ratio is $\mathsf{T}_{ToEpop}/\mathsf{var}_{ToEpop}$ at $\mathsf{ToE}_{\mathsf{pop}}$; and the median of the sensitivity of the population growth rate to climate is $\frac{\partial\lambda}{\partial C_{C=\overline{C}_{CToEpop}}}$. Historical variability is denoted $\mathsf{var}(\lambda_t)$.

	LINEAR				BELL SHAPE			
	F	S_j	S_a	γ	F	S_j	S_a	γ
$\mathsf{ToE}_{\mathsf{pop}}$								
species 1	133	134	125	140	133	126	125	146
species 2	102	64	70	87	106	68	73	86
species 3	116	73	56	63	107	75	60	65
species 4	123	99	54	54	120	105	58	58
$\mathsf{T}_{ToEpop}/\mathsf{var}_{ToEpop}$								
species 1	0.04	0.04	0.04	0.04	0.06	0.04	0.02	0.06
species 2	0.05	0.11	0.09	0.07	0.06	0.11	0.09	0.07
species 3	0.03	0.08	0.15	0.11	0.01	0.08	0.14	0.12
species 4	0.03	0.05	0.16	0.16	0.03	0.03	0.15	0.16
T_{ToEpop}								
species 1	0.0010	0.0032	0.0002	0.0003	0.0041	0.0067	0.0001	0.0085
species 2	0.0010	0.0021	0.0010	0.0008	0.0027	0.0021	0.0011	0.0018
species 3	0.0008	0.0008	0.0008	0.0006	0.0007	0.0010	0.0007	0.0005
species 4	0.0002	0.0004	0.0004	0.0003	0.0005	0.0004	0.0003	0.0002
var_{ToEpop}								
species 1	0.024	0.088	0.003	0.005	0.092	0.216	0.005	0.149
species 2	0.019	0.019	0.011	0.013	0.047	0.021	0.014	0.027
species 3	0.024	0.010	0.005	0.005	0.054	0.013	0.005	0.005
species 4	0.006	0.008	0.002	0.002	0.023	0.020	0.002	0.002
$\frac{\partial\lambda}{\partial C_{C=\overline{C}_{CToEpop}}}$								
species 1	0.010	0.019	0.003	0.004	0.0018	0.0060	0.0002	0.0005
species 2	0.012	0.024	0.011	0.009	0.0022	0.0048	0.0023	0.0021
species 3	0.014	0.009	0.010	0.007	0.0025	0.0019	0.0021	0.0013
species 4	0.001	0.003	0.005	0.004	0.0005	0.0009	0.0011	0.0008
$\mathsf{var}(\lambda_t)$								
species 1	0.025	0.108	0.003	0.006	0.005	0.022	0.001	0.002
species 2	0.019	0.019	0.011	0.014	0.003	0.004	0.002	0.003
species 3	0.031	0.010	0.006	0.005	0.007	0.002	0.001	0.001
species 4	0.008	0.009	0.003	0.002	0.002	0.002	0.001	0.000

Supplementary

Supporting Information S1: population variability in a stationary environment

Equation 13 shows that the variance in annual population growth rates $\mathsf{var}(\lambda_t)$ is linearly related to the climate variance σ^2 in a stochastic stationary environment with small variations around a climate mean $\overline{C}$.

Figure S 1 shows the variance in annual population growth rates $\mathsf{var}(\lambda_t)$ as function of a mean climate $\overline{C}$ for different life histories when climate affects the population through different demographic rates θ_i. The functional relationships between climate and the demographic rate are linear on the real scale for fertilities (except species 4) or on the logit scale for other demographic rates. Let's assume that C represents temperature, and the population is stable for $\overline{C} = 0$.

The stationarity variability of the population growth rate varies as function of the mean climate in complex non-linear ways that depend on $\frac{\partial\lambda}{\partial C}$ and the sign of the slope of the functional relationships between climate and demographic rates β_0 that affects $\frac{\partial\lambda}{\partial C}$. The smallest $\frac{\partial\lambda}{\partial C}$, hence population growth rate variability, occurs for species 4 with an extreme long-lived history and the climate-dependent demographic rate of maturation rate regardless of the mean environmental conditions and functional relationships. Short-lived species (species 1 and 2) and the climate-dependent demographic rate of juvenile survival shows the largest $\frac{\partial\lambda}{\partial C}$, except for extreme positive mean climate. However, various patterns are observed between these extremes, which depend on the functional relationship between climate and demographic rates, the demographic rate by which climate affects population and the life histories of the species.

For example, for linear functional relationships between the fertility and climate (species 1-3), equation 13 becomes:

$$\mathsf{var}(\lambda) = \beta_0^2\sigma^2\left(\frac{\partial\lambda}{\partial\theta_{i_{\theta_i=\overline{\theta_i}}}}\right)^2\left(\frac{\partial\theta_{i_{\theta_i=\overline{\theta_i}}}}{\partial C_{C=\overline{C}}}\right)^2 = \beta_0^4\sigma^2\left(\frac{\partial\lambda}{\partial\theta_{i_{\theta_i=\overline{\theta_i}}}}\right)^2 \tag{14}$$

If $\beta_0 > 0$, $\left(\frac{\partial \lambda}{\partial \theta_i}\right)^2$ increases as $\overline{C}$ increases, and the variance in annual population growth rates is larger for warmer climate than colder climate. If $\beta_0 < 0$, $\left(\frac{\partial \lambda}{\partial \theta_i}\right)^2$ decreases as $\overline{C}$ increases, and the variance in annual population growth rates is larger for colder climate than warmer climate.

For non-linear sigmoid functions, it is more complex, and depends on the specific shape of the $\left(\frac{\partial \lambda}{\partial \theta_i}\right)^2$ and the sign of β_0, specifically at which environment $\overline{C}$ the maximum $\left(\frac{\partial \lambda}{\partial \theta_i}\right)^2$ occurs. For example, for adult survival, the population growth rate variability is larger for warmer climate than for colder climate for long lived species when $\beta_0 < 0$ (species 3 and 4). However, the opposite pattern occurs for short lived species (species 1 and 2): the population growth rate variability is smaller for warmer climate than for colder climate (Fig. S 1). These patterns are opposite when $\beta_0 > 0$.

For bell shape functional relationships, the variance of the population growth rate is smaller for comparable range of demographic rates (Table 2). Indeed, to obtain a realistic range of demographic rates when $\theta_{it} = g(y^* = \beta_0^* C_t^2 + \beta_1 + \epsilon_t)$ than when $\theta_{it} = g(y = \beta_0 C_t^2 + \beta_1 + \epsilon_t)$ (Fig. S 3), the slope of the function y^* must be smaller: $\beta_0^* < \beta_0$. Hence $\mathrm{var}(\lambda)$ is smaller despite similar magnitude for $\left(\frac{\partial \lambda}{\partial \theta_i}\right)^2$ for both function y and y^* (Fig. S 2).

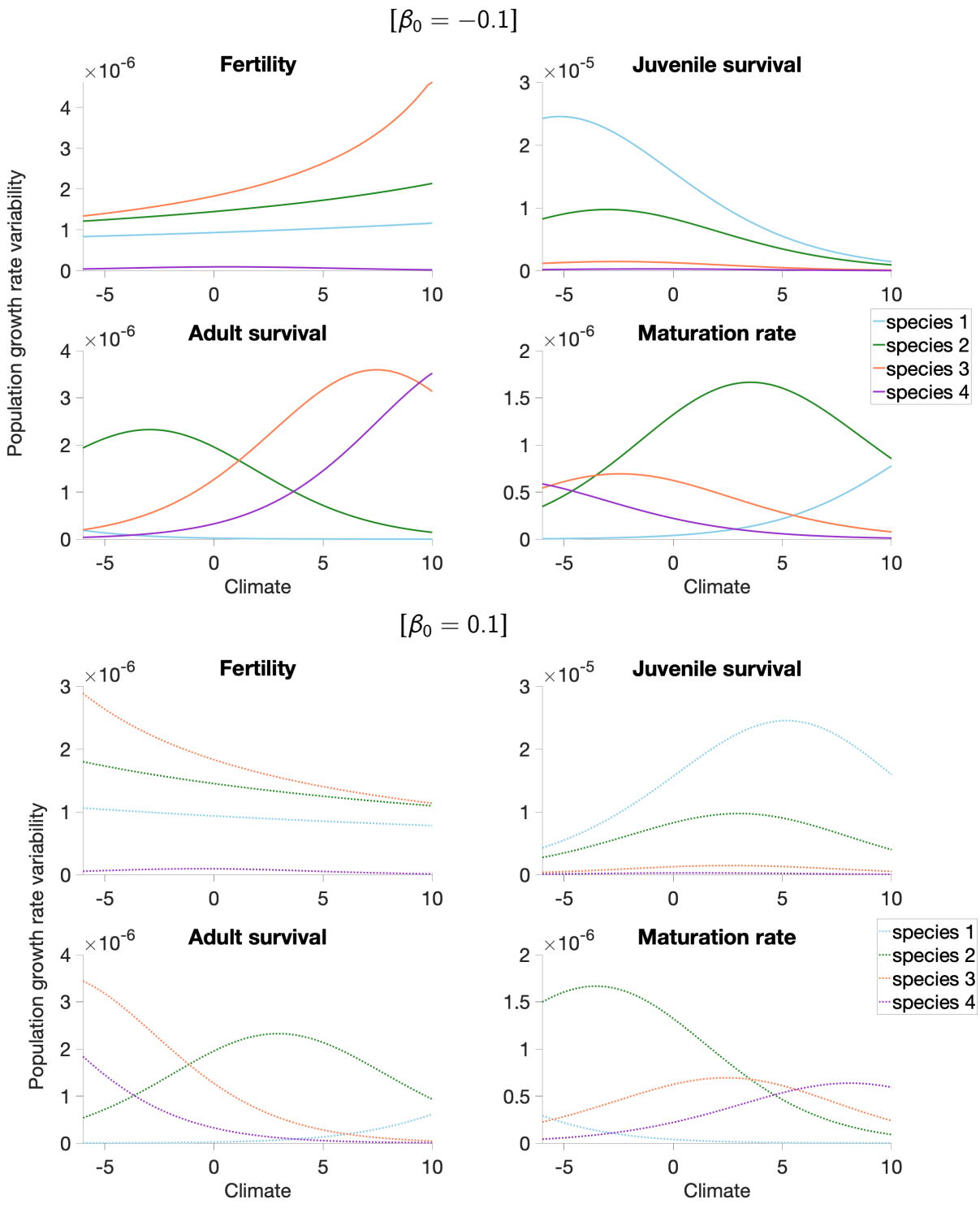

Figure S 1: Variability in annual population growth rates calculated from equation 8 across life histories. Panels show the variance in annual population growth rates var(λ_t) as function of the climate mean $\overline{C}$ when climate affects population through different demographic rates: fertility, survival or maturation. Line color indicates different species along a gradient of fast-slow life histories, from fast (species 1) to slow (species 4). (a) $\beta_0 = -0.1$ and (b) $\beta_0 = 0.1$. $\sigma = 0.2$.

Supporting Information S2: additional figures

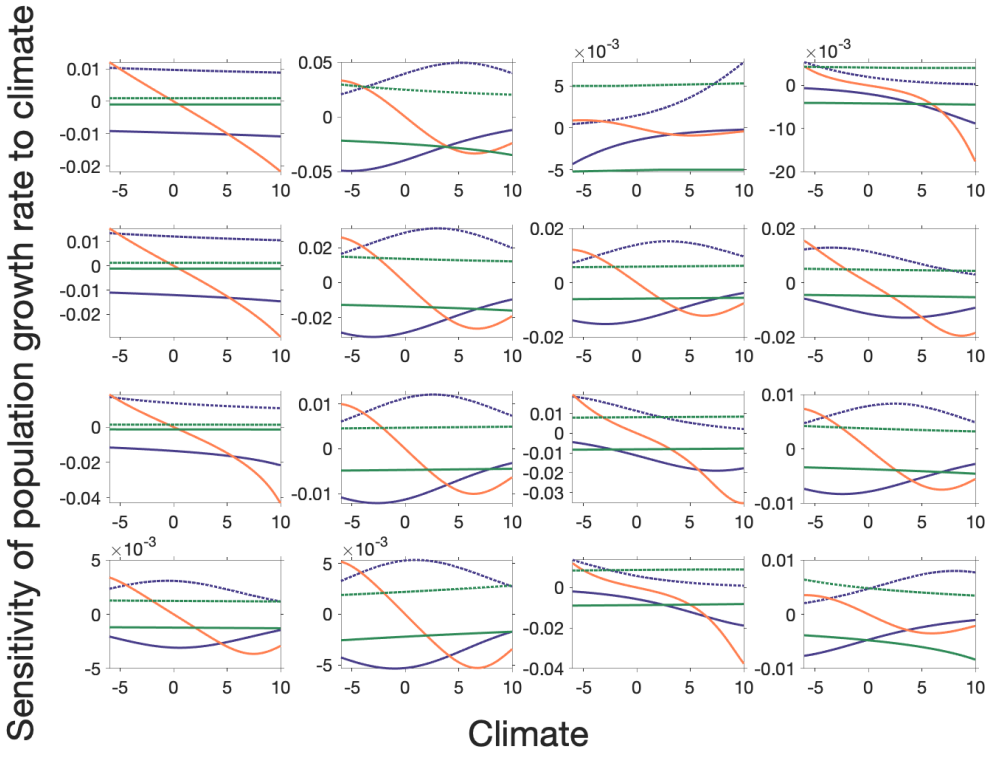

Figure S 2: Sensitivity of the population growth rate to climate for four life histories (panel in line: fast (species 1) to slow (species 4)) and demographic rates (panel in column: fertility, juvenile survival, adult survival and maturation rate) and different functional relationships between climate and demographic rates. Blue lines stands for linear on logit scale with $\beta_0 = [-0.1/0.1]$, orange line shows bell shape on logit scale with $\beta_0 = -0.01$, and green lines are linear on real scale $\beta_0 = [-0.1/0.1]$,

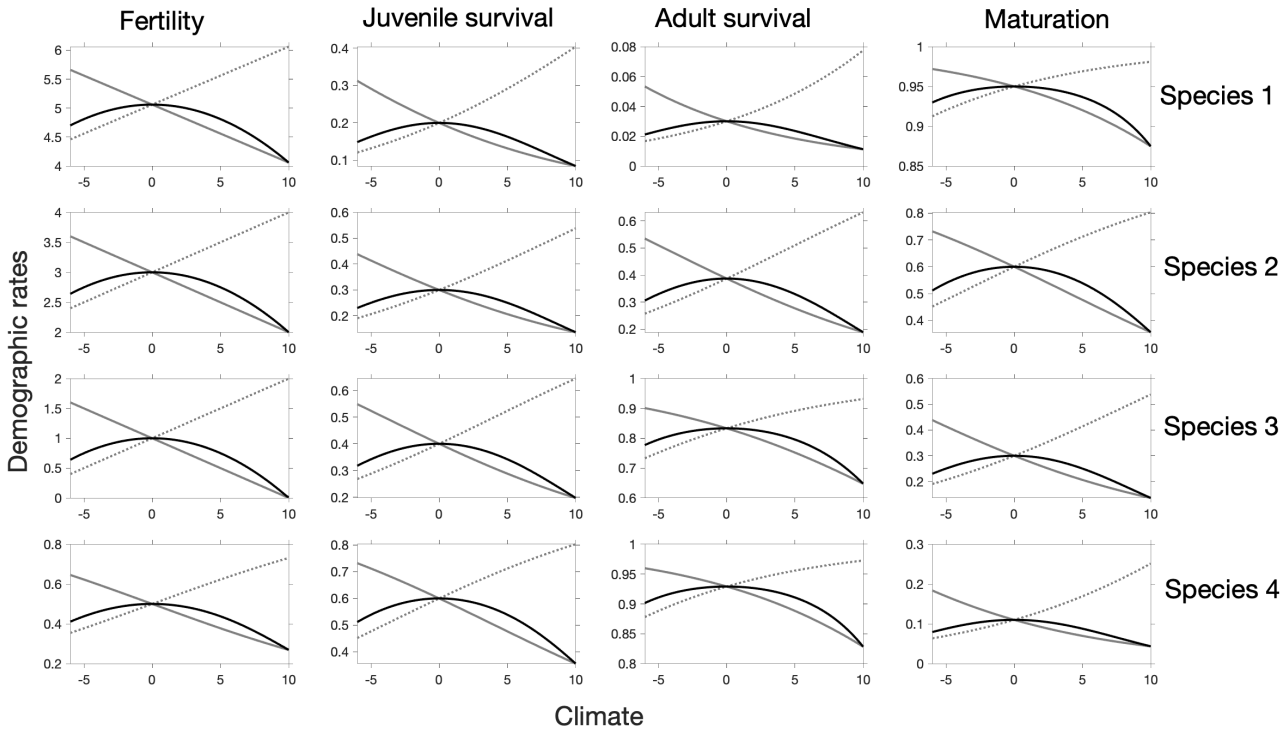

Figure S 3: Example of functional relationships that are linear or sigmoid with a slope $\beta_0 = 0.1$, $\beta_0 = -0.1$ for linear sigmoid functional relationship or $\beta_0 = 0.01$ for bell shape relationships for each species (row panels) and each demographic rate (column panels).

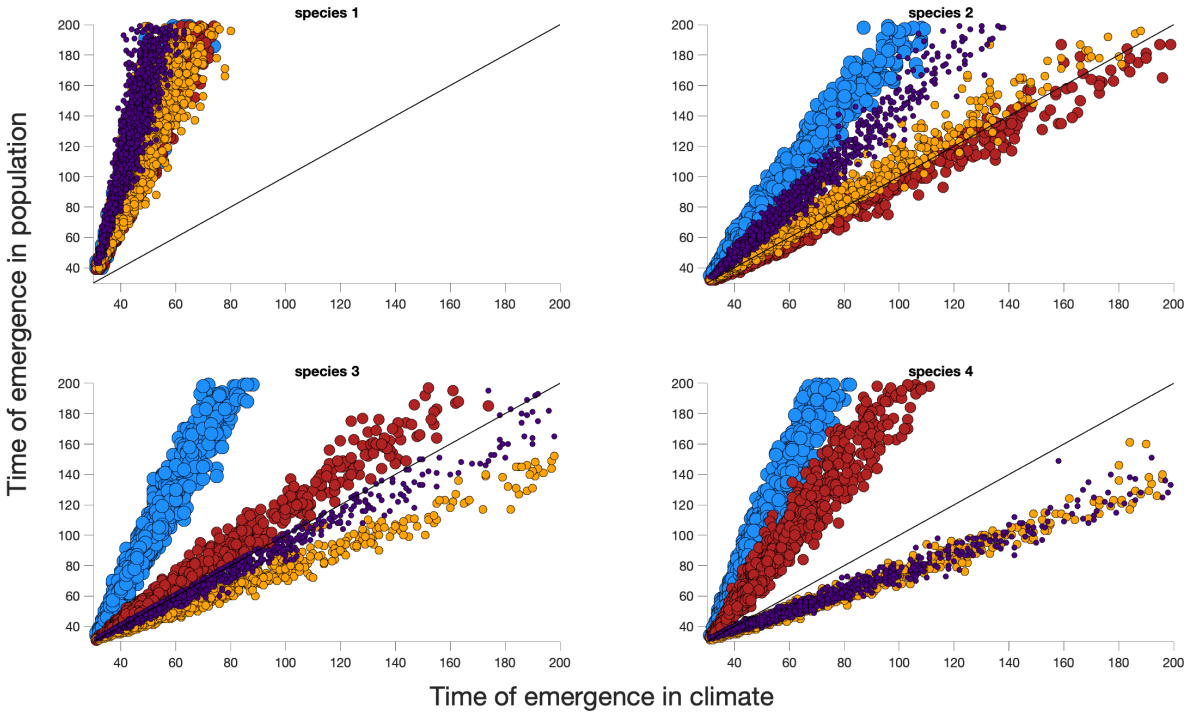

Figure S 4: Relationship between the time of emergence in climate (x-axis) and population (y-axis) for four life history strategies (panels), whereby climate affects only one demographic parameter at a time (colored dots: blue is fertility, red is juvenile survival, orange is adult survival and purple is maturation rate). The black line represent the time when the time of emergence in climate and population are equal. The functional relationships are linear or sigmoid. The emergence thresholds are defined by the 20th or 80th percentile values of the confidence interval. In that case, the system is likely highly sensitive to climate as severe impacts are thought to occur for lower percentile of the climate distribution experienced during the historical run.

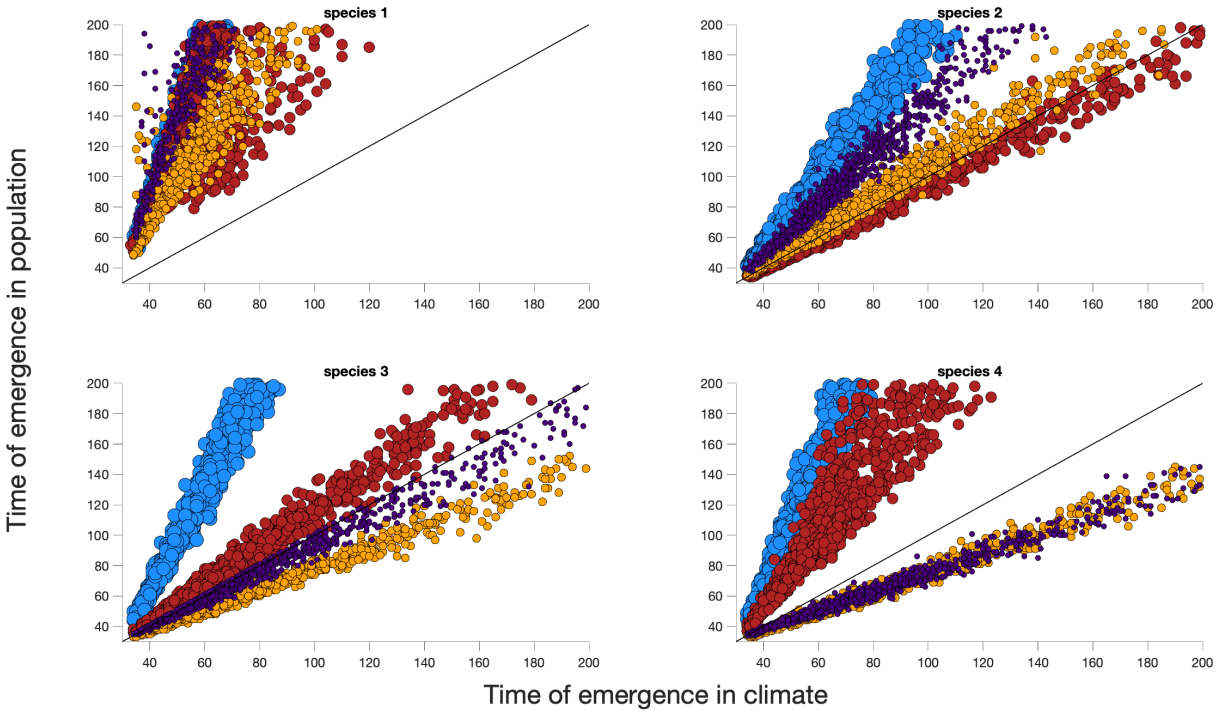

Figure S 5: Relationship between the time of emergence in climate (x-axis) and population (y-axis) for four life history strategies (panels), whereby climate affects only one demographic parameter at a time (colored dots: blue is fertility, red is juvenile survival, orange is adult survival and purple is maturation rate). The black line represent the time when the time of emergence in climate and population are equal. The functional relationships are linear on the real scale with $\beta_0 = [-0.03 \ -0.02 \ -0.01 \ 0.01 \ 0.02 \ 0.03]$.

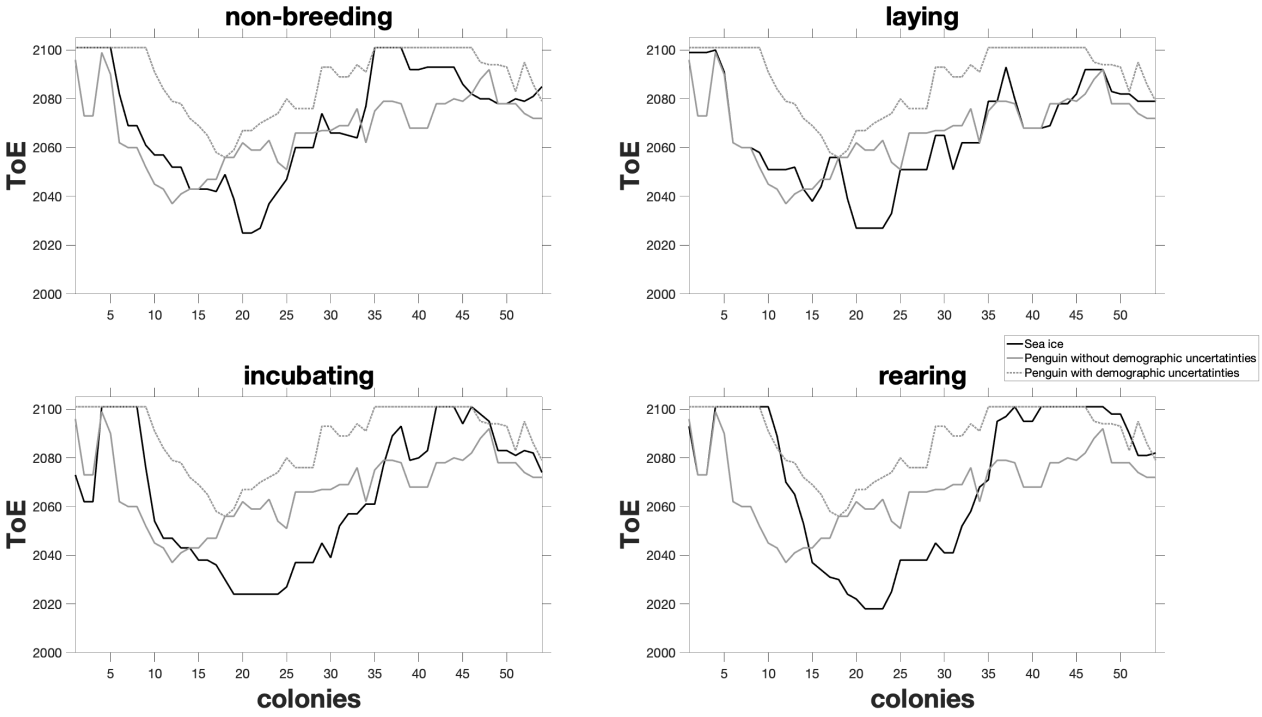

Figure S 6: Time of emergence in sea ice (black line) and in the population growth rate of emperor penguin (grey lines) for the 54 known colonies (x-axis) and season (panels). The calculation of ToE accounts for var(ϵ) generated by parameter uncertainty and process variance (i.e., environmental stochasticity) (dotted line) or not (plain line).

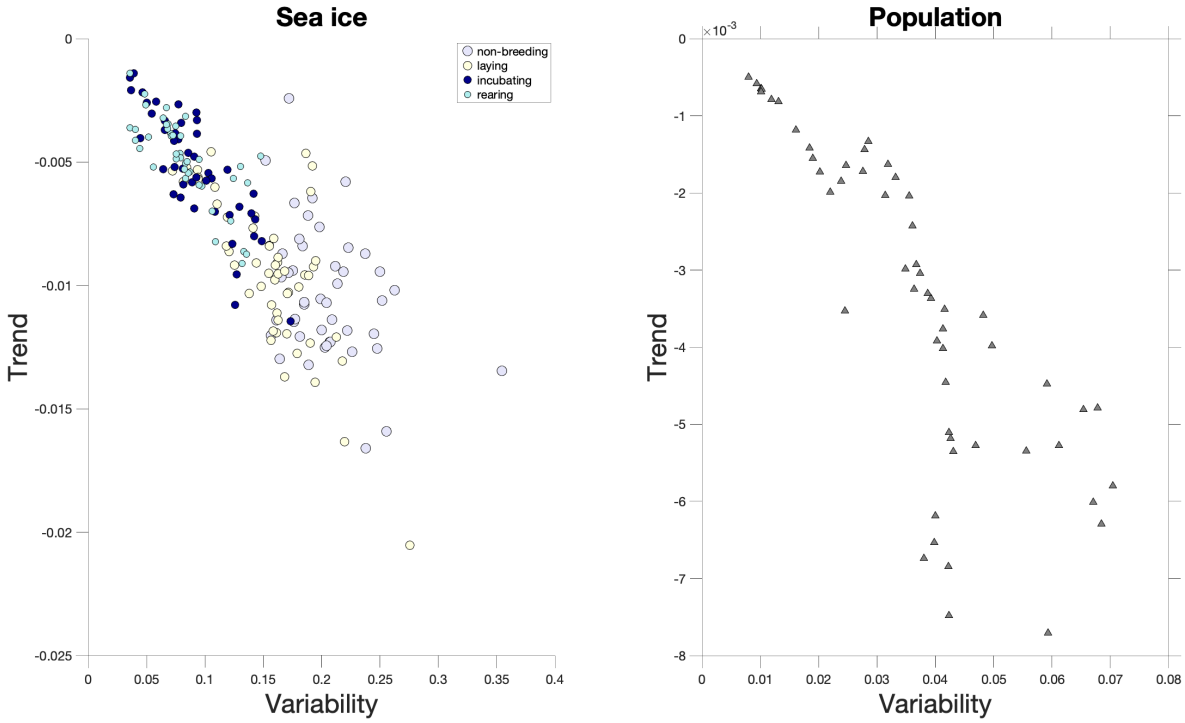

Figure S 7: Variability and trend at the time of emergence for sea ice (left panel) and for the population growth rate of emperor penguin (right panel) for the 54 known colonies (marker) and season (colors).

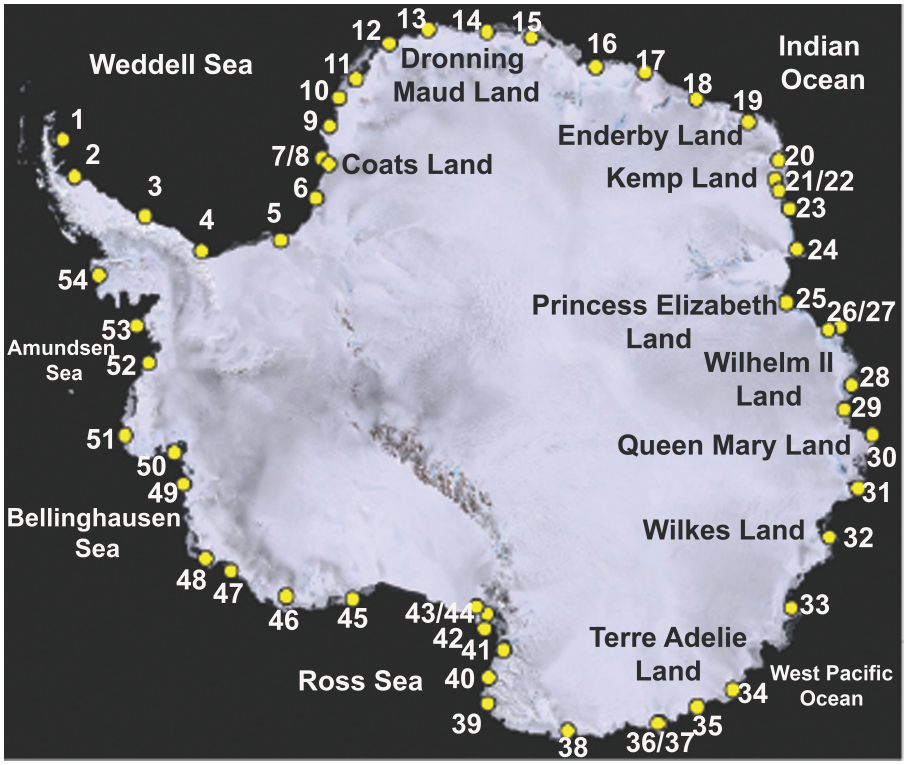

Figure S 8: Map of Emperor penguin colonies.